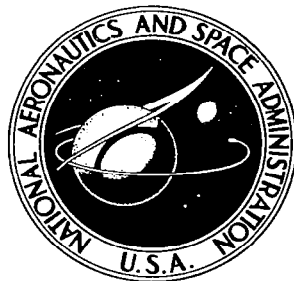# NASA CONTRACTOR REPORT

NASA CR-546

NASA CR-5

N·A·S·A

MINIMAX CONTROL OF LARGE LAUNCH BOOSTERS

by K. D. Graham

Prepared by
HONEYWELL, INC.
St. Paul, Minn.
for George C. Marshall Space Flight Center

NATIONAL AERONAUTICS AND SPACE ADMINISTRATION • WASHINGTON, D. C. • JULY 1966

NASA CR-546

MINIMAX CONTROL OF LARGE LAUNCH BOOSTERS

By K. D. Graham

Distribution of this report is provided in the interest of information exchange. Responsibility for the contents resides in the author or organization that prepared it.

FOREWORD

This document partially comprises the final report prepared by Honeywell, Incoporated for George C. Marshall Space Flight Center, Huntsville, Alabama, 35812 under Contract NAS 8-11206.

NASA CR-547 contains the results of four studies related to the minimax control problem. Two short studies of the effect of non-zero initial conditions on performance and selection of minimax controllers from a given set of controllers were reported. The other two studies present means for determining extremal bounded amplitude, bounded rate inputs to linear systems.

The work on this contract was supervised by Mr. C. R. Stone and Dr. E. R. Rang. This document was prepared by Mr. K. D. Graham and Mr. D. D. Fairchild and Dr. C. A. Harvey contributed to the work.

ABSTRACT

Optimal control theory has been applied to a piecewise constant approximation of a large launch booster for the first 84 seconds of flight. This period was divided into seven intervals with a different constant approximation of the vehicle in each interval. The controllers considered are linear controllers with constant gains in each flight interval. The disturbances are the cross-winds of bounded amplitude which cause the maximum of any of several cost items to occur in each flight interval, and each cost item is proportional to some physical quantity of interest. The cost of a given controller is the maximum of its several cost items.

Optimal control theory provides a straightforward method of computing the cost of a finite set of controllers. The controller of the set with minimum cost is called the minimax controller of that set. It will usually be a sub-optimal controller since the cost computations (called minimax computations) are performed for only a finite set of controllers.

Bending moment is weighted heavily in the cost items for the minimax computations. A comparison of control costs for specific drift-minimum controllers and minimax controllers is presented. It is found that the minimax controllers have lower gains and substantially lower costs than the specific drift minimum controllers considered.

In the material presented, it is shown that one can impose "classical" design criteria on the class of controllers to be considered and still use minimax computations to specify remaining control parameters.

CONTENTS

CONTENTS

TABLES

SECTION I
QUALITATIVE PROBLEM DESCRIPTION

The description of the launch booster studied is provided in a document from M.S.F.C. entitled, Model Vehicle No. 2 for Advanced Control Studies. In this report, the document is referred to as the data package.

The large variations in speed, dynamic pressure, and vehicle characteristics during the first few minutes of powered flight show the importance of considering a time-varying plant.

Using minimax (optimal) control theory, the maximum values of items of importance (e.g., pitch attitude, lateral velocity, gimbal angle, or bending moment) can be computed when the vehicle with a given controller is subjected to the bang-bang disturbance (e.g., cross-wind velocity) which switches sign at the time instants necessary to cause the largest possible response.

Minimax theory in its present state may be applied efficiently to constant coefficient plants, and to time-varying plants by resorting to more expensive computations. The approach reported here has been to divide the first 84 seconds of flight into seven intervals and to approximate the time-varying plant by a different set of constant-coefficient differential equations in each of the seven intervals. The fifth interval contains the event of Mach 1 and the seventh that of maximum dynamic pressure.

One control criterion for large launch boosters is to minimize structural bending. A first approximation to this is to consider the vehicle as a rigid body and design a controller which minimizes the major causes of bending. This approximation is used, and it has the advantage of having a simple formulation; yet it is likely to demonstrate the main features of designing a controller for which minimization of maximum bending moments is weighted heavily as a design criterion.

SECTION II
SUMMARY OF THEORY AND EXTENSION
OF COST FUNCTIONAL

The following optimal control problem is considered. It is assumed that the plant is represented by the vector differential equation:

$$\dot{x} = Ax + Bu + Cg, \quad x(0) = x^o \tag{1}$$

In this equation, x is an n-vector describing the state of the system, x^o is the given initial condition, u is an m-vector representing the control inputs, and g is a k-vector representing the disturbance inputs. A, B, and C are constant matrices of appropriate sizes. Classes of allowable controllers and disturbances are assumed to be as follows: Ω is a class of linear fixed-gain controllers, i.e., $u \epsilon \, \Omega$ if:

$$u = Qx + Rg \tag{2}$$

where Q and R are constant matrices of appropriate sizes; the class of disturbances G is defined by:

$$G = \left\{ g(t) \colon a_i \le g_i(t) \le b_i, \quad a_i \le b_i, \quad i = 1, 2, .., k; \quad t \, \epsilon \, \left[o, T \right], \, g(t) \text{ measurable} \right\}$$

Associated with the class of disturbances G is a constant vector h (the mean disturbance of the class) defined by $h_i = (a_i + b_i)/2$, $i = 1, 2, . . , k$.

To define the performance index, it is assumed that weighting n-vectors d(i) and k-vectors f(i), i = 1, 2,....., s are given, where d(i) and f(i) are independent of t, x^o, and g for each i. For $u \epsilon \, \Omega$, the cost functional C(u) is defined as

$$C(u) = \max_{1 \le i \le s} \, C_i(u) \tag{3}$$

where the <u>cost items</u> $C_i(u)$ are:

$$C_i(u) = \max_{[0,T]} \max_{g \in G} |d(i) \cdot x(t; x^o, u, g) + f(i) \cdot g| \qquad (4)$$

$$i = 1, 2, \ldots, s$$

with $x(t; x^o, u, g)$ representing the solution to (1) with controller (2). An <u>optimal</u> controller is a $u \in \Omega$ which minimizes $C(u)$. A <u>minimax</u> controller is one which minimizes $C(u)$ over the set of u's considered. A minimax controller will in general be sub-optimal since costs C will be determined over only a finite subset of all $u \in \Omega$.

Substitution of (2) in (1) gives the closed-loop equation

$$\dot{x} = A_Q x + C_R g$$

where $A_Q = A + BQ$ and $C_R = C + BR$. Harvey has shown (Refer to Appendix A) that

$$\max_{t \in (o,T)} \max_{g \in G} |d(i) \cdot x(t; x^o, u, g)|$$

$$= \max_{t \in [o,T]} \left\{ |\lambda_i(t)| + \mu_i(t) \right\} \qquad (5)$$

where

$$\lambda_i(t) = \lambda_i(t; x^o, u) = d(i) \cdot e^{A_Q t} x^o + \int_0^t d(i) \cdot e^{A_Q \tau} C_R h \, d\tau \qquad (6)$$

$$\mu_i(t) = \mu_i(t; u) = \sum_{j=1}^{k} \frac{b_j - a_j}{2} \int_0^t |d(i) \cdot e^{A_Q \tau} C_R (j)| \, d\tau \qquad (7)$$

It is seen from (6) that $\lambda(t)$ is independent of individual disturbances $g(t)$, and depends on the mean h of all disturbances. From (7) one sees that the disturbances which maximize (5) have all bang-bang components. At the instant of time t (and corresponding g) for which (7) is maximum, one can change, if necessary, the signs of the components of g without changing the result of the maximizing process for μ_i. Therefore, the values of (4) may be computed by:

$$C_i(u) = \max_{t \varepsilon [0, T]} \left\{ |\lambda_i(t)| + \mu_i(t) \right\} + \max |f(i) \cdot g| \qquad (4A)$$

As also shown in Appendix A, everything necessary for the computation of $\lambda_i(t)$ and $\mu_i(t)$ can be obtained by integrating $n(k + 2) + 2s$ first order differential equations, all but s of which are linear and the remaining s are piecewise linear. The required integration can be readily carried out on a high speed computer.

The cost functional (3) is somewhat more general than the one of the same notation in Appendix A because the term $f(i) \cdot g$ in (4) (equivalently max $|f(i) \cdot g|$ in (4A)) is not considered in Appendix A. This extension of the cost functional was necessary to consider bending moment as a cost item in the formulation of the launch booster problem presented in this paper.

The vectors $d(i)$ and $f(i)$ will be assumed to have the following form:

$$d(i) = D_i \begin{bmatrix} e_1(i) \\ \cdot \\ \cdot \\ \cdot \\ e_j(i) \\ \cdot \\ \cdot \\ e_n(i) \end{bmatrix} \qquad f(i) = D_i \begin{bmatrix} e_{n+1}(i) \\ \cdot \\ \cdot \\ \cdot \\ e_{n+k}(i) \end{bmatrix} \qquad (8)$$

In each i, D_i is constant. For each i and j, $e_j(i)$ may depend on controller gains, flight condition, etc., but not on time.

An important part of the subjective input to the minimax control design procedure is in the choice of the weighting vectors $d(i)$ and $f(i)$. This choice is important since changing a particular weighting vector $d(j)$ and/or $f(j)$ in (4) will alter $C_j(u)$. This may alter the choice of the C_i which is selected in (3) as the cost C, and thus alter the choice of the "best" controller (the one which minimizes C).

The quantities selected for consideration in the control cost functional (3) will govern the selection of the $e_j(i)$'s. The relative weights to be given to each quantity selected are determined by the values chosen for the D_i's. Cases will exist where certain ranges of values on some D_i's will be ineffective. A variety of illustrations appear in Section 5 for a three-dimensional state space (n = 3) to facilitate interpretation.

SECTION III
EQUATIONS OF MOTION AND CONTROLLER FOR
RIGID VEHICLE APPROXIMATION TO LAUNCH BOOSTER

EQUATIONS OF MOTION

A system of second order differential equations which represents the longitudinal motion of a rigid approximation to the launch booster described in the data package with open loop control is as follows:

$$\ddot{\phi} = -\frac{C_{Z_\alpha}}{C_{D_O}} \cdot \frac{X}{I_{xx}} \left(x_{cg} - x_{cp}\right) \left[\phi - \frac{\dot{Z}}{V} + \frac{V_w}{V}\right] - \frac{1}{2} \frac{F}{I_{xx}} \left(x_{cg} - x_\beta\right)\beta$$

(9)

$$\ddot{Z} = \frac{1}{M}\left[F - X\left(1 - \frac{C_{Z_\alpha}}{C_{D_O}}\right)\right]\phi - \frac{C_{Z_\alpha}}{C_{D_O}} \cdot \frac{X}{M}\left[\frac{\dot{Z}}{V} - \frac{V_w}{V}\right] + \frac{1}{2}\frac{F}{M}\beta$$

This system has been linearized by assuming small angle of attack (5 degrees or less). Table 1 describes the symbols used.

The controller class is that of linear fixed-gain controllers of the form:

$$\beta = K_1\phi + K_2\dot{\phi} + \left(\frac{K_3}{V}\right)\dot{Z} - \left(\frac{K_3}{V}\right)V_w \quad .$$

(10)

It is worth digressing momentarily to note that since attack angle α is given by:

$$\alpha = \phi - \left(\frac{\dot{Z} - V_w}{V}\right) ,$$

(11)

(10) is equivalent to a controller using pitch attitude ϕ, pitch rate $\dot{\phi}$, and attack angle α as shown in (10A).

6

Table 1. Table of Physical Quantities

Symbol	Description	Dimension
X	Drag Force	kg
M	Mass	$kg\text{-}sec^2/m$
q	Dynamic Pressure	kg/m^2
V	Vehicle Velocity	m/sec
#	Mach Number	
F	Total Thrust	kg
I_{xx}	Moment of Inertia	$kg\text{-}sec^2\text{-}m$
x_β	Engine Gimbal Point	m
D	Diameter of Vehicle	m
C_{Z_α}	Normal Force Coefficient	
C_{D_o}	Drag Coefficient	
CP	Center of Pressure	m
CG	Center of Gravity	m
$x_{cp} = (CP + x_\beta)$	Station of CP	m
$x_{cg} = (CG + x_\beta)$	Station of CG	m
x_A	Station of Accelerometer	m
A_a	Normal Acceleration	
ϕ	Pitch Attitude Deviation from Reference Trajectory	rad
α	Attack Angle	rad
Z	Displacement Perpendicular to Reference Trajectory	m
M_B	Bending Moment	m-kg
M'_α	Bending Moment Coefficient	m-kg/rad
M'_β	Bending Moment Coefficient	m-kg/rad
V_W	Speed of Wind Perpendicular to Reference Trajectory	m
β	Gimbal Deflection Angle	rad

$$\beta = (K_1 + K_3)\phi + K_2\dot{\phi} - K_3\alpha \qquad (10A)$$

Furthermore, by a more complicated manipulation, (10) can be shown to be equivalent to a linear controller with pitch attitude ϕ, pitch rate $\dot{\phi}$, and normal acceleration A_a feedback, where the normal accelerometer is located at x_A.

Note that it is also assumed that the gimbal motor perfectly reproduces the control signal.

It is necessary to change (9) and (10) into the form and notation of Section II. The state vector x, controller u, and disturbance $g(t, a_i, b_i)$ are defined as:

$$x = \begin{bmatrix} \phi \\ \dot{\phi} \\ \dot{Z} \end{bmatrix} \qquad u = \beta \qquad g = V_w: \quad \begin{aligned} a_1 &= -\left|V_w\right|_{max} \\ b_1 &= +\left|V_w\right|_{max} \\ a_i &= b_i = 0, \ i \neq 1 \\ h_i &= 0, \ \text{all } i \end{aligned}$$

Then define matrices A, B, and C:

$$A = \begin{bmatrix} 0 & 1 & 0 \\[2em] a\dfrac{(x_{c_g} - x_{c_p})}{I_{xx}} & 0 & a\dfrac{(x_{c_g} - x_{c_p})}{I_{xx}}\left(-\dfrac{1}{V}\right) \\[2em] (F - X - a)\dfrac{1}{M} & 0 & a\dfrac{1}{M}\dfrac{1}{V} \end{bmatrix}$$

8

$$B = \begin{bmatrix} 0 \\ -\dfrac{F}{2}\dfrac{(x_{c_g} - x_\beta)}{I_{xx}} \\ \dfrac{F}{2}\dfrac{1}{M} \end{bmatrix} \qquad\qquad C = \begin{bmatrix} 0 \\ a\dfrac{(x_{c_g} - x_{c_p})}{I_{xx}\,V} \\ -a\dfrac{1}{M}\dfrac{1}{V} \end{bmatrix}$$

where $a = -\left[\dfrac{C_{Z_\alpha}}{C_{D_O}}\right] X$

It can be shown (most simply by direct verification) that equation (12) is equivalent to the open loop equations (9) written in the form of equation (1):

$$\dot{x} = Ax + B\beta + CV_w \tag{12}$$

Direct comparison of (2) and (10) shows that

$$Q = \begin{bmatrix} K_1 & K_2 & \dfrac{K_3}{V} \end{bmatrix}$$

$$R = -\dfrac{K_3}{V} \tag{13}$$

It is desirable to employ conventional notation before writing the closed loop form of (12) and (13). Table 2 contains the details of the notation for A, B, and C. The resulting closed-loop equation $\dot{x} = A_Q x + C_R V_w$ where $A_Q = A+BQ$ and $C_R = C+BR$ is given as follows:

9

$$a = - \frac{C_{Z_\alpha}}{C_{D_O}} X$$

$a_{11} = 0$ $\qquad\qquad$ $a_{12} = 1$ $\qquad$ $a_{13} = 0$

$$a_{21} = \frac{a \left(x_{cg} - x_{cp} \right)}{I_{xx}} \qquad\qquad a_{22} = 0 \qquad a_{23} = -a_{21}$$

$$a_{31} = (F - X - a) \frac{1}{M} \qquad\qquad a_{32} = 0 \qquad a_{33} = \frac{a}{M}$$

$b_1 = 0$ $\qquad\qquad\qquad\qquad\qquad$ $c_1 = 0$

$$b_2 = - \frac{F}{2} \frac{\left(x_{cg} - x_\beta \right)}{I_{xx}} \qquad\qquad\qquad c_2 = -a_{23} = a_{21}$$

$$b_3 = \frac{F}{2} \frac{1}{M} \qquad\qquad\qquad\qquad\qquad c_3 = -a_{33}$$

$$
\begin{bmatrix} \dot{\phi} \\[2mm] \ddot{\phi} \\[2mm] \ddot{Z} \end{bmatrix} = \begin{bmatrix} 0 & 1 & 0 \\[2mm] a_{21}+b_2K_1 & b_2K_2 & (a_{23}+b_2K_3)\left(\frac{1}{V}\right) \\[2mm] a_{31}+b_3K_1 & b_3K_2 & (a_{33}+b_3K_3)\left(\frac{1}{V}\right) \end{bmatrix} \begin{bmatrix} \phi \\[2mm] \dot{\phi} \\[2mm] \ddot{Z} \end{bmatrix} + \begin{bmatrix} 0 \\[2mm] (c_2-b_2K_3)\frac{1}{V} \\[2mm] (c_3-b_3K_3)\frac{1}{V} \end{bmatrix}\!V_w
$$

$$\tag{14}$$

Solutions $x(t; x^o, \beta, V_w)$ of (14) are those which appear in the cost functional (5). The definition of the disturbance class (just preceding 12) simply says that the cross-winds can blow equally hard in either direction. As a result, the vector h is identically zero so that the integral term in (6) makes no contribution to cost.

The first term in (6) depends on initial conditions x^o and is non-zero only when one or more state vector components are initially non-zero. All the computations reported in this document had zero initial conditions on each interval, so $\lambda_i(t) = 0$ for all i and all t.

LUES OF COEFFICIENTS

Inspection of Table 2 shows that the following coefficients and the values of velocity are sufficient to describe all time-variable elements of (14):

$$a_{21},\ a_{31},\ a_{33},\ b_2,\ b_3\ .$$

The most striking variation with time is observed by plotting $\frac{a_{21}}{V} = \frac{-a_{23}}{V}$. This is shown in the top half of Figure 1 as a broken-line graph connecting the points eight seconds apart for which all information was available from the data package. The horizontal line segments show the seven intervals into which the first 84 seconds of flight were subdivided, and the corresponding values of $\frac{a_{21}}{V}$ over the interval spanned by each segment. The intervals and values were chosen by inspection of the graph.

The values of a_{21} (Figure 2, top) were chosen in the same manner over the same subintervals. Then the values of V (Figure 4, bottom) were chosen to make the selected values of $\frac{a_{21}}{V}$ and a_{21} consistent in each subinterval. The values of the remaining coefficients and dynamic pressure q were selected by graphical inspection and the results are shown in Figures 1 through 4. One value was used in two or more of the later intervals for a_{31}, a_{33}, b_2, and b_3, since these graphs did not have such wide variation as a_{21}.

The values of wind velocity magnitudes are shown in Table 3. The values are calculated from information in the data package.

Table 3. Wind Velocity Magnitudes

Interval	Time (sec)	$\left|V_w\right|_{max}$ (m/sec)
I_1	0-20	13.5
I_2	20-36	19.5
I_3	36-52	31
I_4	52-60	44.5
I_5	60-68	59
I_6	68-76	75
I_7	76-84	75
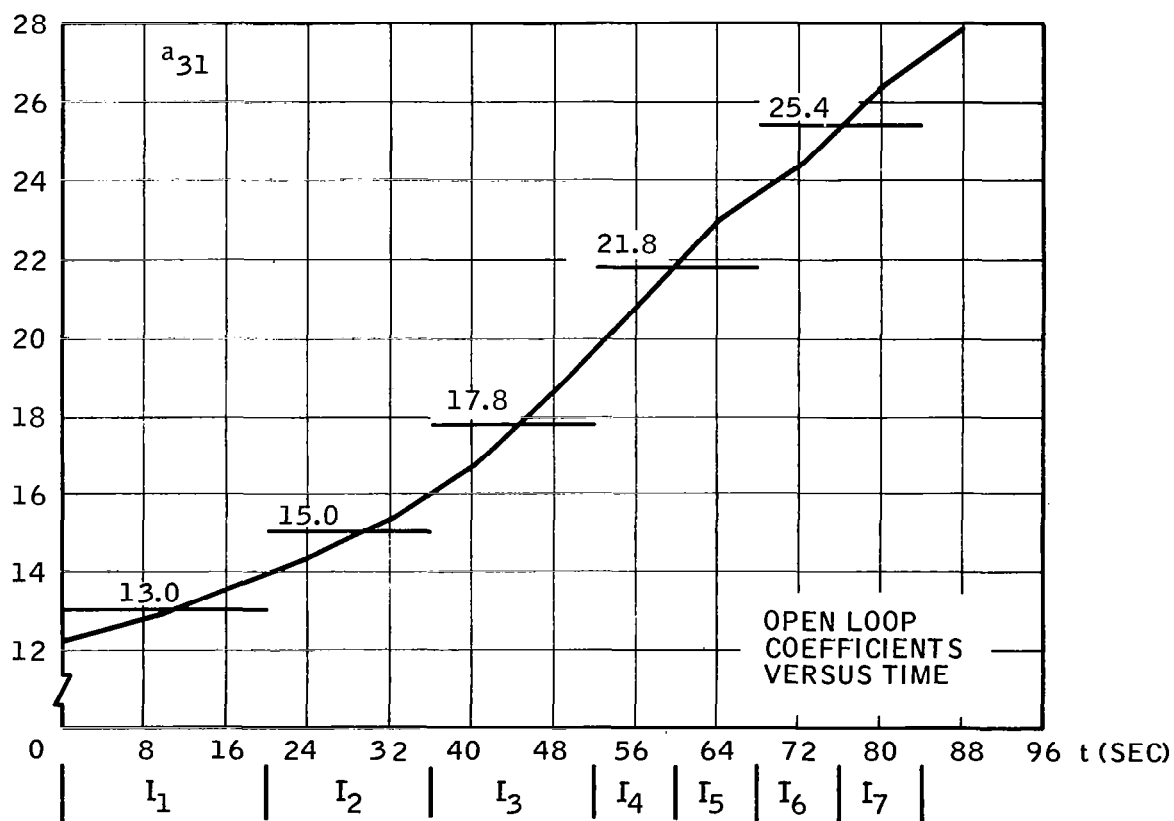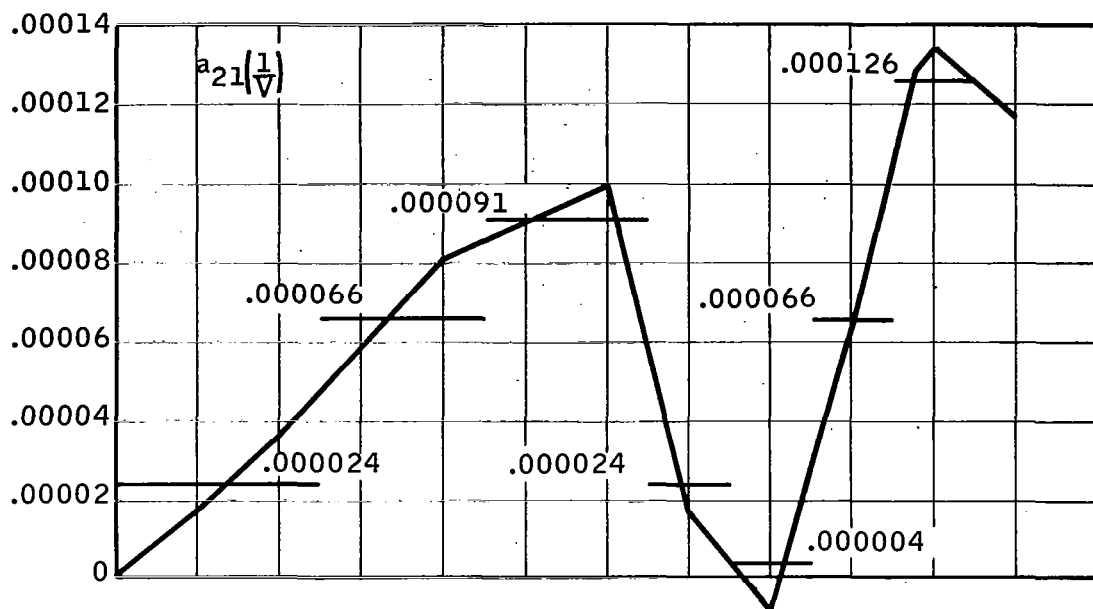
Figure 1. Open-Loop Coefficients vs Time
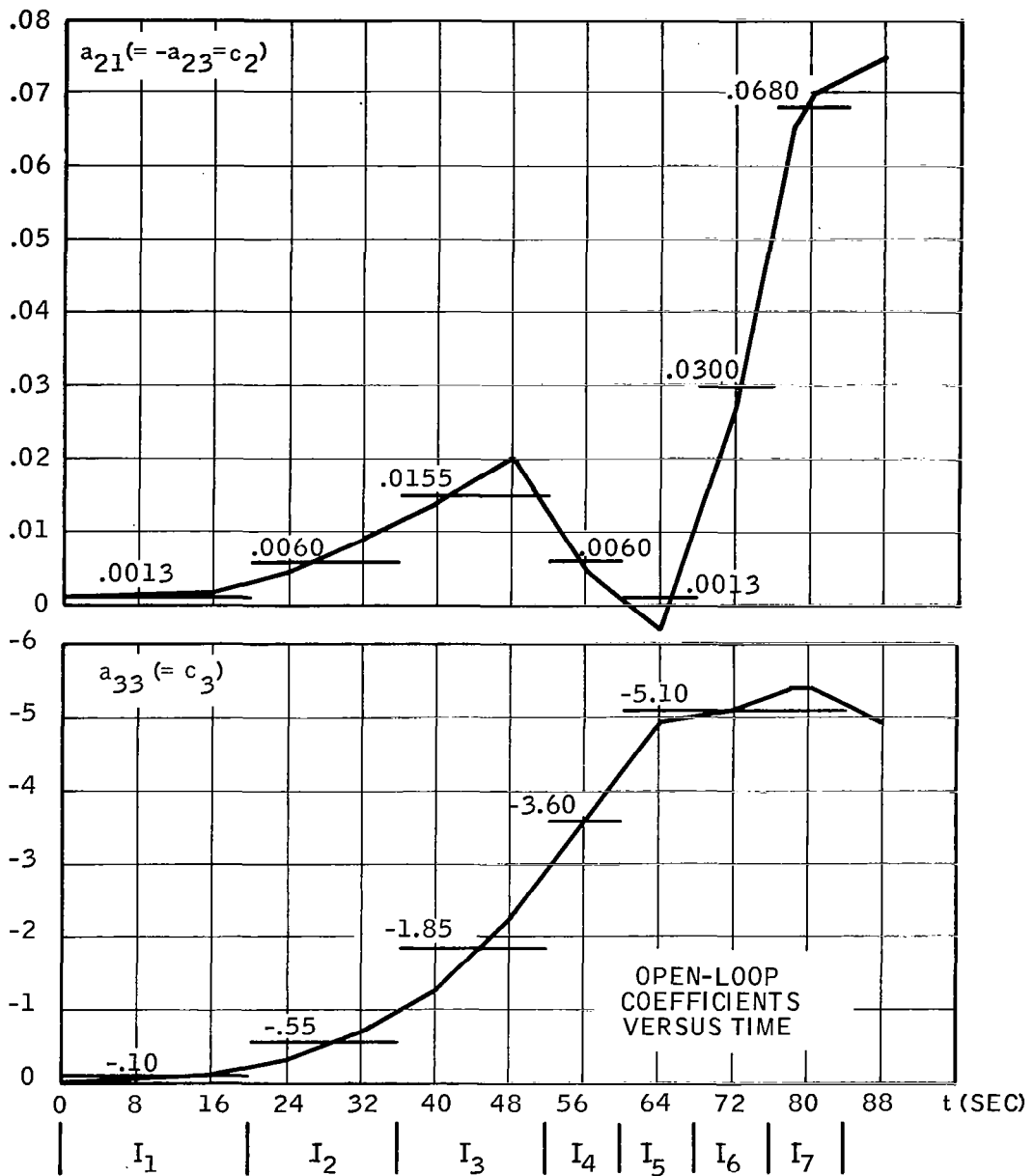
Figure 2. Open-Loop Coefficients vs Time
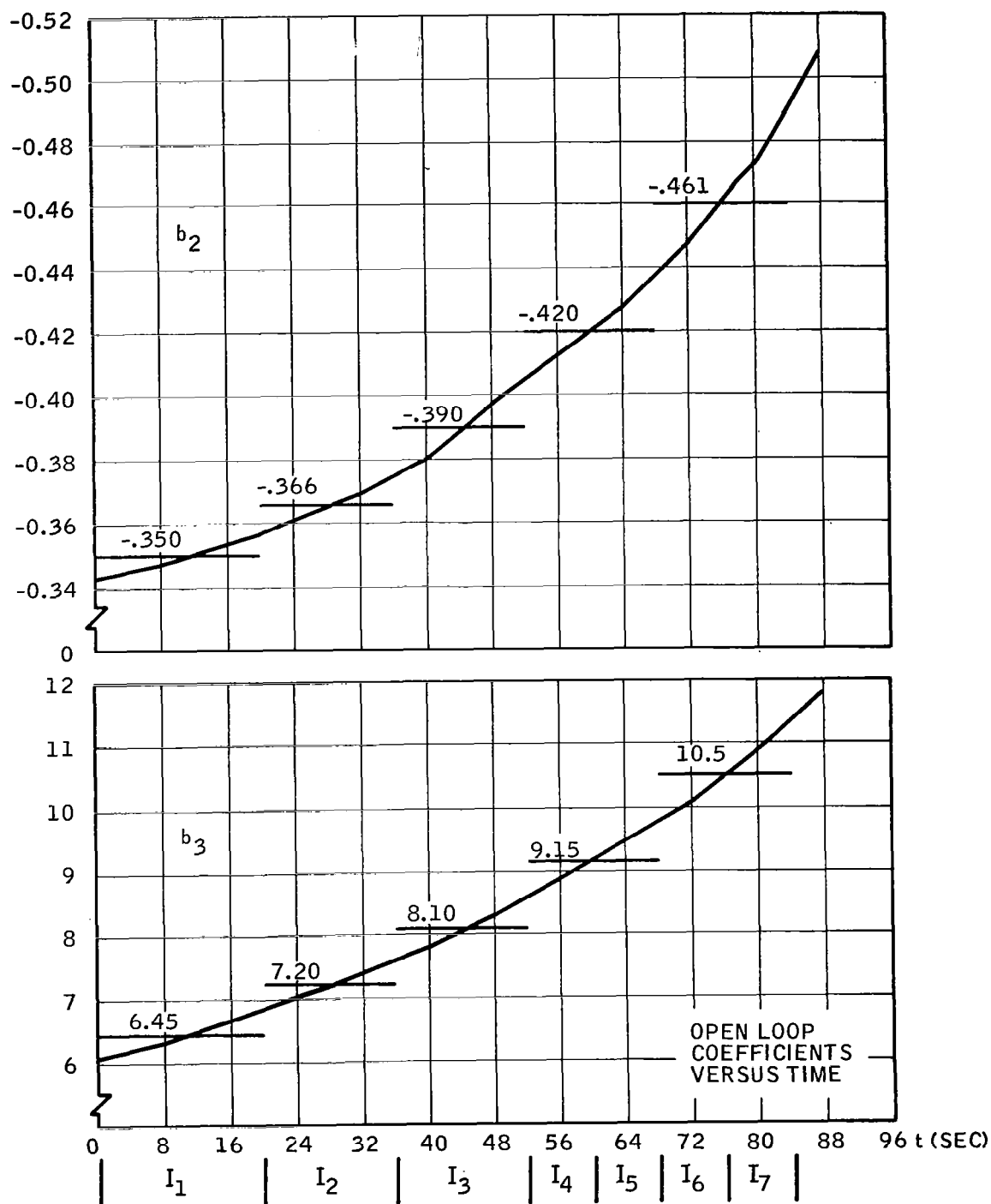
Figure 3. Open-Loop Coefficients vs Time
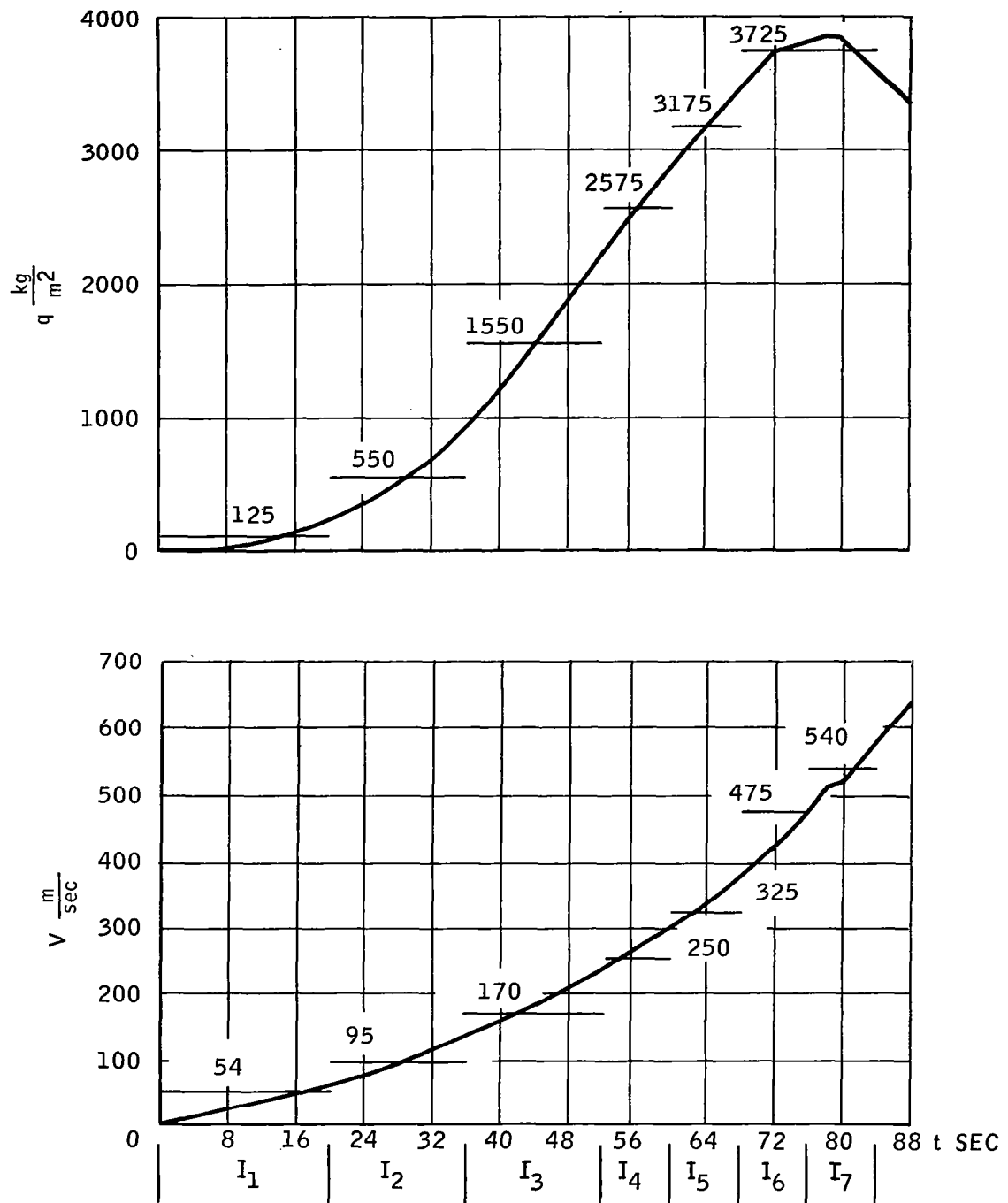
Figure 4. Open-Loop Coefficients vs Time

SECTION IV
BENDING MOMENT

The formulation of bending moment, its value as a control criterion, and estimates of peak bending moment coefficients are given in this section.

BENDING MOMENT FORMULATION

One control criterion for large launch boosters is to minimize structural bending. The bending moments are caused by:

- Engine gimbal deflection

- Non-zero angle of attack

- Influence of bending itself on local angle of attack

- Fuel slosh

The first two items are the major causes of bending moments. The third is relatively small and is absent until some bending has been caused by another source. Bending moments due to fuel slosh are small. Hence, bending moments depend primarily on engine gimbal deflection and attack angle, and will be assumed to have the following representation:

$$M_B = (M_\alpha')\alpha + (M_\beta')\beta \tag{15}$$

The values of the coefficients M_α' and M_β' depend on the longitudinal location on the vehicle and other factors which vary with time (the most important ones will be stated later in this section under headings: M_α' at CG versus Time and M_β' at CG versus Time). Figure 5 shows M_α' and M_β' at $t = 72$ and $t = 78$ for
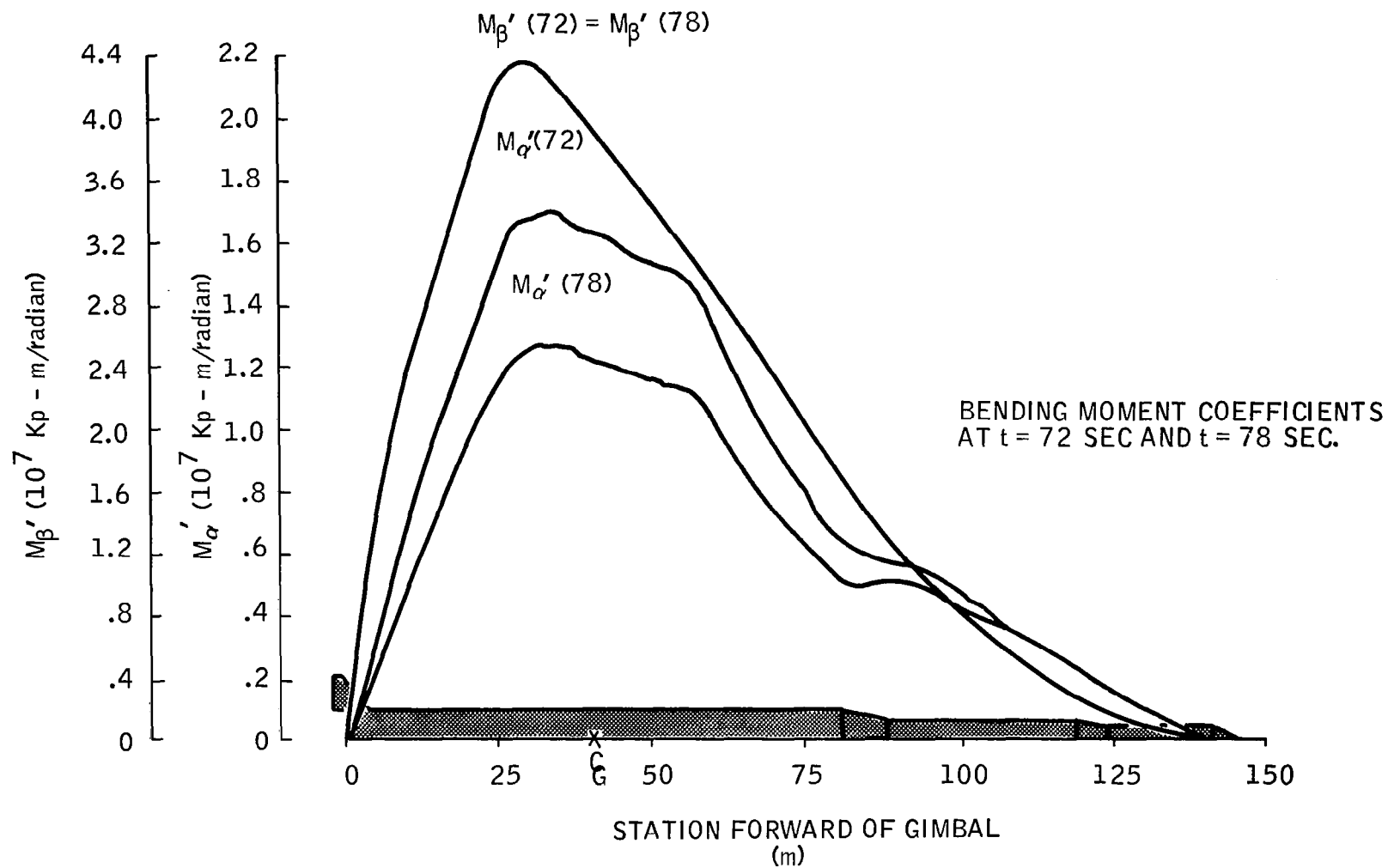
Figure 5. Bending Moment Coefficients at t = 72 Sec. and t = 78 Sec.

the data package vehicle. Positions along the vehicle are measured by stations, each one meter long, numbered consecutively from zero at the engine gimbal to about 150 at the nose. Note that both M_α' and M_β' have peak values approximately at station 35 (near the center of gravity) and taper more or less smoothly to zero at each end of the vehicle.

BENDING MOMENT -- A CONTROL CRITERION

Since the basic idea of minimax control of large launch boosters is to protect the structure, it would be preferable to minimize the ratio of bending moment to structural stiffness; i.e., minimize $M_B/(EI)$. The EI distribution for Model Vehicle No. 2 has sharp relative minima of EI (i.e., weak spots) in zones about four meters long centered at about stations 23 and 50. The values of the ratios $M_\alpha'/(EI)$ and $M_\beta'/(EI)$ near these two stations exceed their corresponding values at station 35, where M_α' and M_β' themselves are maximum, by a factor of only about 1.6. Thus, minimizing only bending moment M_B at any particular station or minimizing peak bending moment achieves about the same result as minimizing $\max\limits_{\text{all stations}} [M_B/(EI)]$. The gain from either approximation is a simple control criterion.

ESTIMATES OF BENDING MOMENT VERSUS TIME

Estimates of M_B were needed for the whole interval $0 \leq t \leq 84$. During this interval, the CG of Model Vehicle No. 2 moved from station 37.5 to 42, the peak value of M_β' moved from station 33 to 30, and the peak value of M_α' remained between stations 34 and 40 except for a short time in the third flight interval when the peak of M_α' occurred near station 56. It was assumed that for $0 \leq t \leq 84$, the peak values of M_α' and M_β' occurred at the same station (later specified as the CG) and the control criterion chosen was that of minimizing this peak value of M_B.

M'_α at CG versus Time

Figure 5 shows that the values of M'_α (72) exceed those of M'_α (78) by a sig-
nificant amount. An elementary analysis indicates that M'_α ought to be
somewhat proportional to dynamic pressure q. Since dynamic pressure
has its peak value at t = 78, rather than at t = 72, it is seen that elementary
theory is not suitable for approximation beyond t = 72.

It was assumed that M'_α at the CG was proportional to q and inversely pro-
portional to I_{xx} in the interval $0 \leq t \leq 72$, with values normalized to
$M'_\alpha\big|_{t=72} = 1.70 \times 10^7$ m-kg/rad. In the interval $72 \leq t \leq 78$, M'_α at the CG
was obtained by linear interpolation between the peak values of M'_α shown in
Figure 5. For $78 \leq t \leq 84$, $M'_\alpha = M'_\alpha\big|_{t=78}$. The resulting graph is shown in
Figure 6, together with the constant approximating values used in the seven
flight intervals.

M'_β at CG versus Time

It was assumed that M'_β at the CG was proportional to thrust magnitude F
and inversely proportional to longitudinal moment of inertia I_{xx}, with values
normalized to $M'_\beta\big|_{t=78} = 4.32 \times 10^7$ m-kg/rad. Figure 7 shows the resulting
graph of M'_β at the CG versus time, together with the constant approximating
values used in the seven flight intervals.

COLLECTION OF ASSUMPTIONS ON BENDING MOMENT

The significant assumptions on bending moment are summarized here. Bending
moment was computed according to Equation (12). Peak values of M'_α and M'_β
at each instant of time (either given or estimated as described earlier in this
section under headings: M'_α at CG versus Time and M'_β at CG versus Time)
were used. Thus, an estimate of the peak bending moment on the structure

20
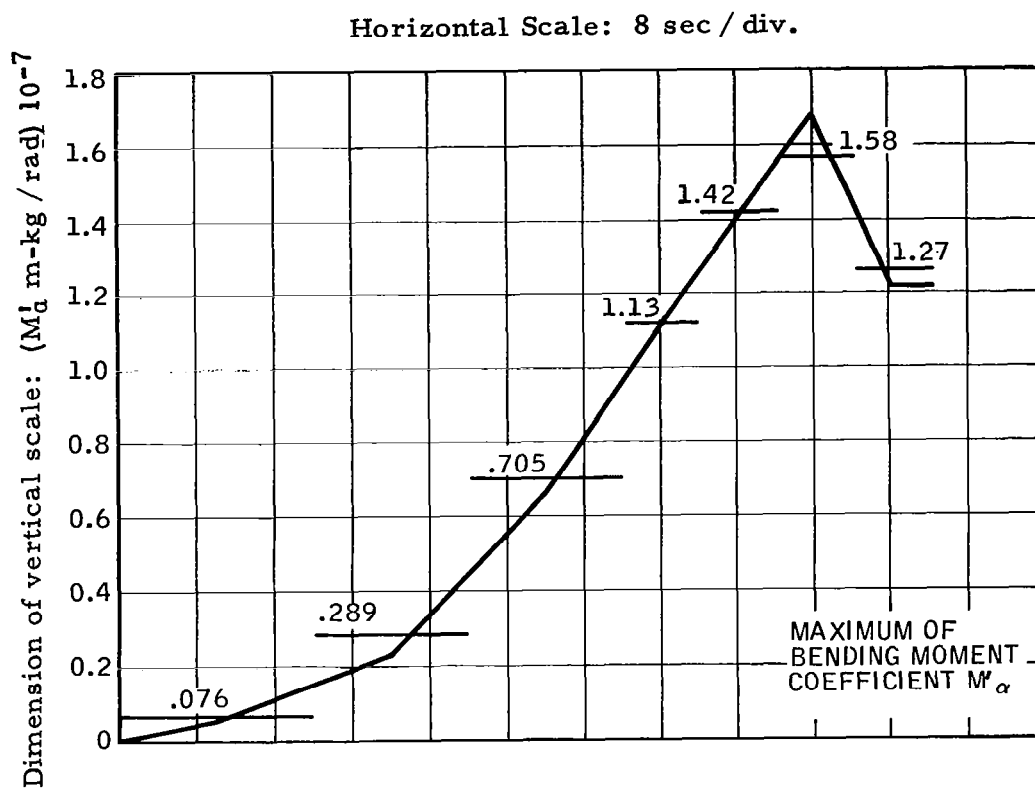
Figure 6.   Maximum of Bending Moment Coefficient M'α
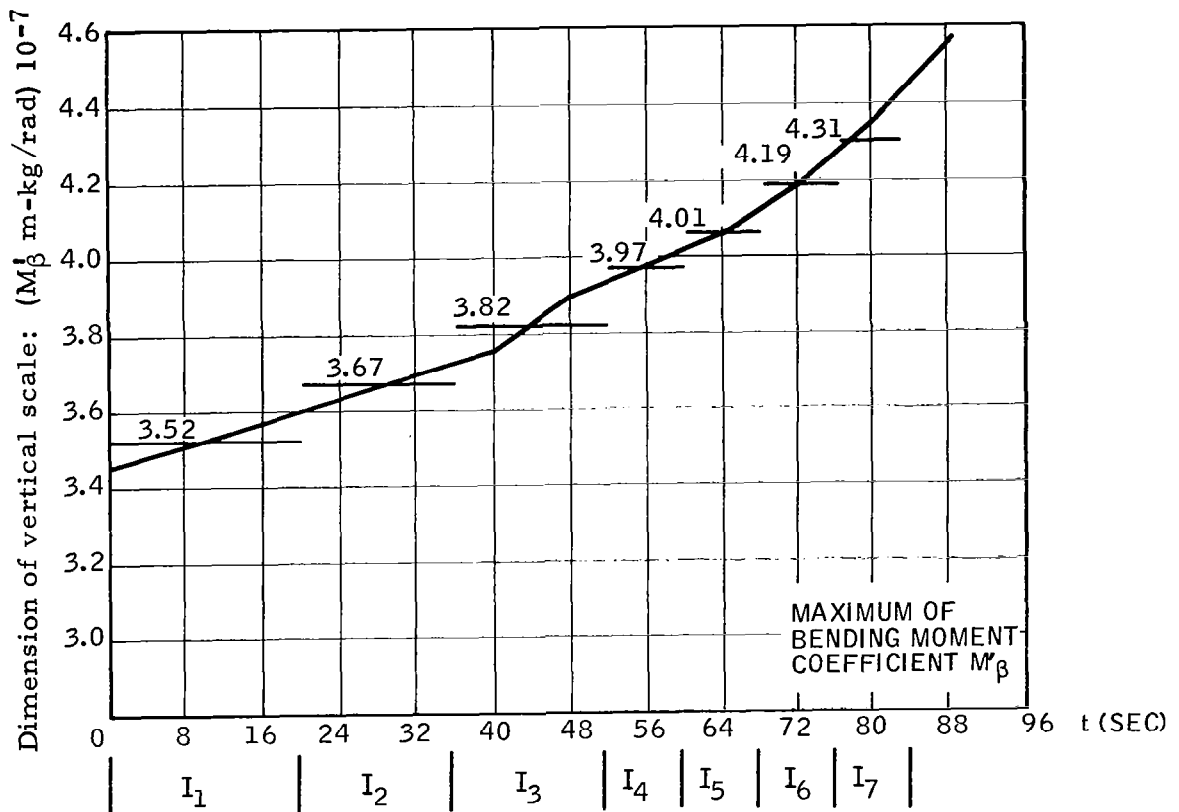
Figure 7. Maximum of Bending Moment Coefficient $M'\beta$

at each instant of time was used in formulating control criteria. It is of interest to note that supplementary data on peak values of M'_α and M'_β which was received too late to be used in the computations shows the assumptions outlined under headings M'_α at CG versus Time and M'_β at CG versus Time to be substantially correct, although the values of M'_β should have been more nearly constant.,

BENDING MOMENT IN THE NOTATION OF SECTION II

Bending moment can be expressed in terms of state variables and disturbance winds V_w by substituting (10) and (11) into (15) for β and α respectively. The result is (15A).

$$
M_B = \left[(M'_\alpha + K_1 M'_\beta) \quad\quad K_2 M'_\beta \quad\quad \frac{(-M'_\alpha + K_3 M'_\beta)}{V} \right] \begin{bmatrix} \phi \\ \dot{\phi} \\ \dot{Z} \end{bmatrix}
$$

$$
+ \frac{(M'_\alpha - K_3 M'_\beta)}{V} V_w
$$

(15A)

This equation shows explicitly how bending moment will depend on the controller gains K_1, K_2, K_3.

CHOICE AND INTERPRETATIONS OF
WEIGHTING VECTORS

To facilitate interpretation of the weighting vectors $d(i)$ and $f(i)$ defined in (8), additional notation conventions will be adopted. Recall that: 1) n is the number of components in the state vector (i.e., n is the dimension of the state space), 2) each $d(i)$ is an n-vector, 3) each $f(i)$ is a k-vector, and 4) there is a total number s of each (i.e., $i = 1, 2, \ldots, s$). Assume that $s \geq n$ so that there are at least as many cost elements C_i as the dimension of the state space. Then assume that the first n of the $d(i)$'s and $f(i)$'s are the weighting vectors for the state variables taken individually. More complicated cost criteria will be assigned index values $i > n$.

INTERPRETATION OF $d(i)$, $f(i)$, $i = 1, 2, \ldots, n$

To weight only a particular state variable x_i, begin by defining (in (8))

$$e_i(i) = 1 \qquad i \leq n$$

$$e_j(i) = 0 \qquad j = 1, 2, \ldots, n+k, \ j \neq i.$$

This choice of $e_j(i)$'s merely selects the state variable x_i as the one to be considered.

A simple and illustrative method of weighting x_i is to require that for a <u>given</u> value N of the control cost C, the amplitude of x_i should not exceed some specified amount $|x_i|_{max}$. This is easily accomplished by selecting the scalar D_i according to the rule:

$$D_i = \frac{N}{|x_i|_{max}} \tag{16}$$

Thus, the forms of d(i) and f(i), $1 \le i \le n$, which give cost C = N when x_i has maximum amplitude $|x_i|_{max}$ is

$$d(i) = D_i \begin{bmatrix} 0 \\ \cdot \\ \cdot \\ \cdot \\ 0 \\ 1 \\ 0 \\ \cdot \\ \cdot \\ \cdot \\ 0 \end{bmatrix} \begin{matrix} \\ \\ \\ \\ \\ \text{i-th row} \\ \\ \\ \\ \\ \end{matrix} \qquad \text{and} \quad f(i) = 0$$

where D_i is given by (16).[*]

Figure 8 illustrates the result on a three-dimensional state space of selecting d's and f's in this manner, but some general notation is retained. All cost elements C_i, $1 \le i \le n$ for points $x = (x_1, \cdots, x_i, \cdots, x_n)$ inside the box are less than the specified cost N. Points on the face of the box normal to the x_i axis have one cost element C_i which is equal to N. Points on an edge have two cost elements with value N and all three C_i's are equal to N at the corners of the box. Thus, a controller which keeps all state variables in or on the box is one whose control cost C does not exceed the chosen value N.

Note that the dimension of the box in the i-th direction is inversely proportional-to D_i [see (16)]. Increasing the value of D_i has the effect of reducing the maximum amplitude of the state variable x_i that can be allowed by a controller whose cost C is not to exceed N. Alternately, increasing D_i increases the cost item C_i associated with state variable x_i for a given set of

---

[*] There may be cases where it is not permissible for a given state variable to have the same maximum amplitude in both directions. For example, maximum down-elevator deflection on an aircraft may be more restricted than is up-elevator deflection. This situation can be handled by biasing the value of x_i used in equations 4 and 16.
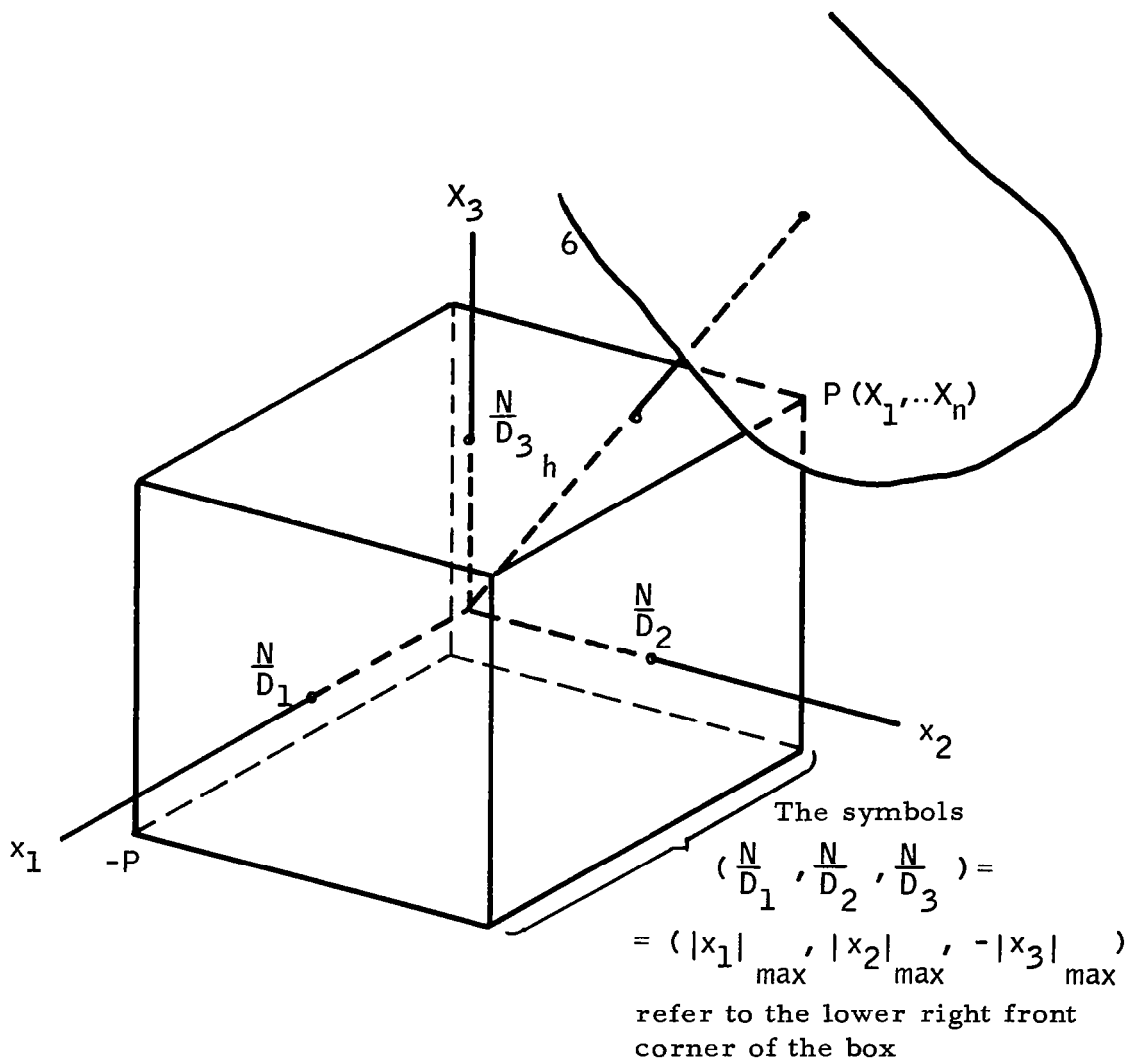
Figure 8. State Space Box Determined by Control Cost N and Weighting Scalars D_i

controller gains. Thus, a larger D_i gives a larger weight to x_i in determining control cost C.

Finally, if no restriction is to be placed on x_i in determining an acceptable controller, simply let D_i = 0. The effect is to stretch the state space box to infinite length in the x_i direction.

INTERPRETATION OF $d(i)$, $f(i)$, $n \leq i \leq s$

Control cost elements C_i, $n < i \leq s$, which are linear combinations of two or more state variables will restrict the state space for a given cost N if D_i is large enough. We will give a method of computing the smallest possible D_i which puts further restrictions on the state space box (illustrated in Figure 8 for $n = 3$) and a given control cost $C = N$.

As an example, consider the cost element C_i, $i > n$, which is associated with a control law u given by (17).

$$u = \sum_{j=1}^{n} K_j x_j \tag{17}$$

The $e_j(i)$'s are specified according to the rule

$$\begin{aligned} e_j(i) &= K_j, \qquad j = 1, 2, \ldots, n \\ e_j(i) &= 0, \qquad j = n+1, \ldots, n+k \end{aligned} \tag{18}$$

Then $f(i) = 0$ and the argument in (4) is simply $|d(i) \cdot x|$. As with state variables, it is common to specify a maximum value $|u|_{max}$ for the control (for example, $|u|_{max}$ may be allowable gimbal deflection). The $|d(i) \cdot x|$ in the cost item C_i has the following form [where notation has been kept general rather than using the non-zero values for $e_j(i)$ given in (18)]:

$$|d(i) \cdot x| = |D_i \sum_{j=1}^{n} e_j(i) x_j| = |D_i u|$$

If D_i is chosen as before, i.e.,

$$D_i = \frac{N}{|u|_{max}} , \tag{19}$$

we again have $C_i = N$ when $|u| = |u|_{max}$.

It remains to see what this cost item does in the way of restricting the state space box. The control $u = \sum_{j=1}^{n} e_j(i) x_j$ defines a family of parallel planes* in the state space. The two planes which represent maximal control are given by

$$\sum_{j=1}^{n} e_j(i) x_j \pm |u|_{max} = 0 \tag{20}$$

Noting (19) and (20), it is seen that these two planes correspond to a cost item $C_i(u) = N$ and can be written as

$$\sum_{j=1}^{n} e_j(i) x_j \pm \frac{N}{D_i} = 0 \tag{21}$$

The two planes of the same family which pass through corners P and -P of the state space box of cost N or less (Figure 8) are represented by

$$\sum_{j=1}^{n} e_j(i) x_j \pm h = 0 \tag{22}$$

---

*The word "plane" has been used throughout, rather than the correct term "hyperplane".

where h is the distance from the origin to these planes (a formula for computing h is given in (25)). Comparing (21) and (22) one sees that control planes of cost N pass through corners of the state space box of cost N if $h = N/D_i$. If $N/D_i > h$, the planes of maximal control ((20) and (21)) lie outside the box. If $N/D_i < h$, the maximal control planes cut corners off the box and further restrict the state space which was established by allowing cost N or less on individual state variables. Therefore, all values of D_i, $i > n$, which satisfy (23) put further restrictions on the state space box of cost N.

$$D_i > \frac{N}{h} \tag{23}$$

There remains the need for computation of h. Let $P = P(X_1, \cdots, X_n)$ denote one of the corners of interest on the state space box. It is clear from (16) and from Figure 8 that $|X_j| = |x_j|_{max} = N/D_j$, $j = 1, 2, \cdots, n$.

The usual formula for the distance h to the plane through $P = P(X_1, \cdots, X_j, \cdots X_n)$ is

$$h = \frac{\left| \sum\limits_{j=1}^{n} e_j(i) X_j \right|}{\left(\sum\limits_{j=1}^{n} e_j^2(i) \right)^{1/2}} \tag{24}$$

But, we know only $|X_j|$ and must determine its sign in order to compute h. This is done simply by noting that the direction numbers of the normal to every plane of the family are $e_j(i)$ so that _all_ X_j's will have either the _same_ or the _opposite_ sign of the direction number with corresponding subscript. Thus, each summand in the numerator of (22) is either positive or negative. Therefore, without knowing the sign of X_j, h may be computed as follows:

$$h = \frac{\displaystyle\sum_{j=1}^{n} |e_j(i)\, X_j|}{\left(\displaystyle\sum_{j=1}^{n} e_j^2(i)\right)^{1/2}} \tag{25}$$

COST ITEMS DEPENDING ON STATE VARIABLES AND DISTURBANCES $n < i \leq s$

Cost items which depended on a linear combination of two or more state variables were considered in the preceding section. It is frequently necessary to consider disturbances in control cost items also. For example, crosswind velocity V_w occurs in both the controller equation (10) and the bending moment equation (15A) in the formulation of the launch booster problem of this report. In such cases, the f's are no longer zero. As an illustration, assume that bending moment is to be considered in the $(n + 2)$-th cost item. Since $n = 3$ and $k = 1$ in this example, we have

$$e_1(5) = M_\alpha' + K_1 M_\beta'$$

$$e_2(5) = K_2 M_\beta'$$

$$e_3(5) = -(M_\alpha' + K_3 M_\beta')/V$$

$$e_4(5) = (M_\alpha' + K_3 M_\beta')/V$$

and

$$d(5) = D_5 \begin{bmatrix} M_\alpha' + K_1 M_\beta' \\ K_2 M_\beta' \\ -(M_\alpha' + K_3 M_\beta')/V \end{bmatrix}, \quad f(5) = D_5 \left[(M_\alpha' + K_3 M_\beta')/V \right]$$

The additional cost due to consideration of non-state variables is given by the last term of (4A); that term is $\max |f(i) \cdot g|$ in general notation and $\left| \left[(M_\alpha' + K_3 M_\beta')/V \right] V_{w_{max}} \right|$ in the case of bending moment. This additional cost should simply be omitted in considering the effects of a particular $d(i)$ on the state space box of cost N (the vector $f(i)$ does not affect it). The computations of the preceding section then apply directly.

INTERPRETATION OF COST ITEMS DEFINED BY (4) AND COMPUTED BY (4A)

The cost items defined by (4) and computed by (4A) can now be conveniently interpreted by a third equation. It has been shown that the $e_j(i)$'s serve to select the quantity of interest and that the D_i's determine the weights to be given the individual quantities. Thus, if y_i denotes a quantity of interest, the corresponding cost item C_i has the meaning shown in (26).

$$C_i = \max_{[0,T]} \max_{g \epsilon G} |D_i y_i| \tag{26}$$

If one agrees to remember that each cost item has been maximized by the worst disturbance of the assumed class for that particular quantity, and that the cost item has also been maximized over the finite time interval of interest, then some of the notation of (26) can be suppressed to give the simple formula (27). This form

$$C_i = D_i |y_i|_{max} \tag{27}$$

has already been suggested by (16) and (19).

WEIGHTING VECTORS AND SCALARS SELECTED

Five cost items were selected for the problem outlined in Sections III and IV. Table 4 shows the items (in the notation of (27), together with the definitions of $e_j(i)$'s and D_i's. Values of V for the fourth and fifth columns of $e_3(i)$ and $e_4(i)$ are obtained from the bottom half of Figure 4. Values of M_α' and M_β' for the fifth column of the $e_j(i)$'s come from Figures 6 and 7, respectively.

Data was supplied by Marshall Space Flight Center which included responses of Model Vehicle No. 2 to wind disturbances when equipped with a drift-minimum controller. The "synthetic wind profiles" (as described in Appendix A of the data package) had peak velocities at 40, 48, 56, 64, 72, 80, and 88 seconds. Two cases were considered for the flight interval containing $t = 48$, one with gusts and one without. The values of the weighting scalars D_i were selected for each flight interval so that maximum responses of the vehicle for wind profiles appropriate to that interval all had the same cost. Then the resulting bending moment weights D_5 were doubled, while the others were left unchanged. The bottom half of Table 4 shows the D_i's for each flight interval. D_2 was initially chosen as zero (so $C_2 = 0$) since explicit pitch rate responses were not given. D_2 was later given a small weight ($D_2 = 0.01$) in order to obtain non-zero values of cost item C_2 and consequently be able to compute maximum pitch rates.

The method of choosing the D_i's accomplished two objectives:

- The method distributed the weights with some recognition of physically realistic values, and

- The method enabled the resulting cost items to be compared directly and interpreted against a known allowable number (e.g., if $D_i = \dfrac{1}{|y_i|_{max}}$, then $D_i \cdot |y_i| \leq 1$).

Table 4. Cost Items and Weight Vectors

i	1	2	3	4	5
y_i*	ϕ rad	$\dot{\phi}$ rad/sec	$\dot{Z}$ m/sec	β rad	M_B m-kg
$e_1(i)$	1	0	0	K_1	$M'_\alpha + K_1 M'_\beta$
$e_2(i)$	0	1	0	K_2	$K_2 M'_\beta$
$e_3(i)$	0	0	1	K_3/V	$-(M'_\alpha + K_3 M'_\beta)/V$
$e_4(i)$	0	0	0	$-K_3/V$	$(M'_\alpha + K_3 M'_\beta)/V$
Scalar Interval	D_1	D_2**	D_3	D_4	D_5
I_1	0.978	0 / 0.01	0.0342	1.56	0.674×10^{-7}
I_2	0.978	0 / 0.01	0.0342	1.56	0.398×10^{-7}
I_3	0.645	0 / 0.01	0.0262	0.838	0.166×10^{-7}
I_4	0.529	0 / 0.01	0.0188	0.684	0.120×10^{-7}
I_5	0.499	0 / 0.01	0.00859	0.763	0.104×10^{-7}
I_6	0.415	0 / 0.01	0.0143	0.608	0.0928×10^{-7}
I_7	0.493	0 / 0.01	0.0314	0.469	0.1072×10^{-7}

*$C_i = D_i |y_i|_{max}$

**When $D_2 = 0$, then $C_2 = 0$. If $C_2 \neq 0$, then $D_2 = 0.01$.

SECTION VI
ITERATIVE INITIAL USE OF MINIMAX COST COMPUTATIONS

INTRODUCTION

The minimax theory gives a computation procedure for identifying the combination of controller gains for which the cost of control of a linear system subjected to maximum disturbance inputs is minimum. A systematic use of this computation procedure is desirable. One procedure that has been evolved is described here. The method amounts to evaluating control costs for a selected set of controllers, and then using this information to select a new set of controllers, some of which have costs less than any in the preceding set. Several iterations of this procedure have been found useful in that each iteration has yielded controllers whose costs were lower than any previously considered controller. Each controller was employed for only one of the seven flight intervals. The duration of each interval ranged from 8 to 20 seconds. At any state of iteration of minimax computations, the minimax controller for a given interval is the one of those considered with the lowest control cost.

The primary goal was to study the applicability of minimax theory to selection of controllers, so no restrictions (such as asymptotic stability) were placed on the class of controllers to be considered and no attempt was made to devise automatic numerical techniques of determining lowest cost controllers. Some consideration of restricting the class of possible controllers is contained in Section IX, but no computations were done with such restrictions employed.

THE PROBLEM CONSIDERED

The mathematical model used was the same as outlined in Sections III and IV. The controller class is defined by (10) and a particular controller is therefore specified by three values of the gains K_1, K_2 and K_3. The following discussion is directly applicable to this situation, but n-dimensional notation is employed with geometric examples shown in three dimensions.

It will be assumed that the control criteria and weighting vectors have been chosen so that cost elements $C_i(u)$ of (4) are defined. The gain space $\mathcal{K}$ is the n-dimensional space whose points K are the n-tuples of numbers K_j, $j=1, 2, \ldots, n$ which comprise one combination of controller gains:

$$(K_1, K_2, \ldots, K_n) = K \in \mathcal{K}.$$

A controller is assumed to be completely specified by selecting a point K. Thus, it is not ambiguous to speak interchangeably of a controller $u = u(K)$ and a point K in gain space $\mathcal{K}$.

The problem at hand is outlined as follows:

    i)   For each $K \in \mathcal{K}$ (i.e., for each combination of controller gains) there are s cost elements C_i, $i=1, 2, \ldots, s$ and the largest one is the cost $C(u)$ of that controller.

    ii)   The cost $C(u)$ is determined by different cost elements $C_i(u)$ in various parts of the gain space $\mathcal{K}$.

    iii) It is desired to locate the point K for which C is minimum.

A PROCEDURE

The <u>first objective</u> of this procedure is to establish a region in the gain space $\mathcal{X}$ which contains the low cost controllers in its <u>interior</u>. The <u>second objective</u> of the procedure is to search the interior of the region for the best controller.

Minimax design calculations were carried out for seven subintervals of the powered flight of a (third order linearized) large launch booster. It was noted in Section III that the coefficients were constant in each interval and that the coefficient matrices of the vehicle's equations of motion were substantially different from one interval to another. The experience gained in these calculations led to the following procedure:

1. Choose a first set of gains $K^1 = (K_1^1, \ldots, K_n^1)$ by any reasonable means.

2. Pick a box in gain space of generous size by selecting a couple of values of each gain on both sides of those in K^1. Use all combinations of the selected values to define a grid of points uniformly distributed in the box.

3. Compute the cost of control for the points of this first grid and see where a few of the lowest cost controllers fit in the grid.

4. If any particular gain K_j is inside the box for the low cost controllers, this seems to be an indication of a somewhat critical range of values for that gain, and a second grid with a refinement and reduced range of values in the j-th direction in gain space should be selected and the computations repeated.

Interior Refinement

It is reasonable to expect that at some stage of grid refinement, the lowest cost controller lies inside the most recent gain box. Assuming that a cost reduction or gain change criterion has not yet indicated completion of attempts at improvement, an interior refinement procedure has been evolved. It consists of picking a reduced range for each gain and establishing a grid which has this lowest cost controller on its interior. Repeating the cost computations is a means of conducting a search for a better controller in the vicinity of the best previous controller.

It is conceivable that interior refinement would be required in the vicinity of several different controllers which were not particularly close together in the gain space $\mathcal{K}$. Limited experience indicates that it is more likely that several good controllers are clustered together and that an interior refinement is conducted in a box which contains all of them.

A graphical technique has been found helpful in choosing refined grids in particularly critical cases. It is discussed in the section entitled Cost Mapping.

Summary of Experience

Before going on, the experience for the example studied will be summarized. The criteria which were adopted for considering a grid refinement to be complete were that decrease in cost and/or the changes in gains from the most recent grid should not exceed 10 percent.

Three gains were involved in the case considered. In attacking the first objective, an initial point $K^1 = (K_1^1, K_2^1, K_3^1)$ in $\mathcal{K}$ was chosen based on gains supplied by Marshall Space Flight Center for a drift minimum controller of a similar vehicle. The gains K_j represent feedback gains for

pitch attitude ϕ, pitch rate $\dot{\phi}$, and lateral velocity $\dot{Z}$, respectively. An initial box in $\mathcal{K}$ was chosen as the box centered at the origin of $\mathcal{K}$ whose sides were of length $4K_1^1$, $4K_2^1$, and $4K_3^1$. Figure 9 illustrates this original box of controllers with K^1 inside of it.

Five values were chosen for each controller gain K_j. They were $K_j = 0$, $K_j = \pm K_j^1$, and $K_j = \pm 2K_j^1$, where $j = 1, 2, 3$. All combinations of these values represent a grid of 125 controllers which lie at the corners of the little boxes subdividing the initial box (see corner A in Figure 9). The costs for these controllers were computed for each of the seven flight intervals and a few of the lowest cost controllers for each interval were selected for further study (Refer to Table 5). The cost elements C_i, $i = 1, 2, 3, 4, 5$, represented respectively the following variables: 1) pitch attitude ϕ, 2) pitch rate $\dot{\phi}$, 3) lateral velocity $\dot{Z}$, 4) gimbal angle β, and 5) bending moment M_B. A strong pattern was immediately apparent. The maximum values of K_1 and K_2 and the zero value of K_3 were very popular among the low cost controllers and the controlling cost was almost always on lateral velocity (C_3). This was not surprising since the method of choosing D_3 would inherently weight lateral velocity rather heavily. Only interval 7 is exceptional to this summary, in that the cost was on bending moment (C_5) and K_3 was negative.

Since the best controllers were clustered near the front and right faces of the box at about zero height (Figure 9), and since the only non-zero values of K_3 which were selected were negative, a second box of about the same size and subdivisions was chosen with its center closer to K^1. (It was at (4.5, 10, -0.7)). These results are in Table 6 and can be summarized in exactly the same way: Maximum values of K_1 and K_2 and zero values of K_3 were popular with the low cost controllers, and the cost was almost always on lateral velocity (C_3). In interval 7, the negative value of K_3 closest to
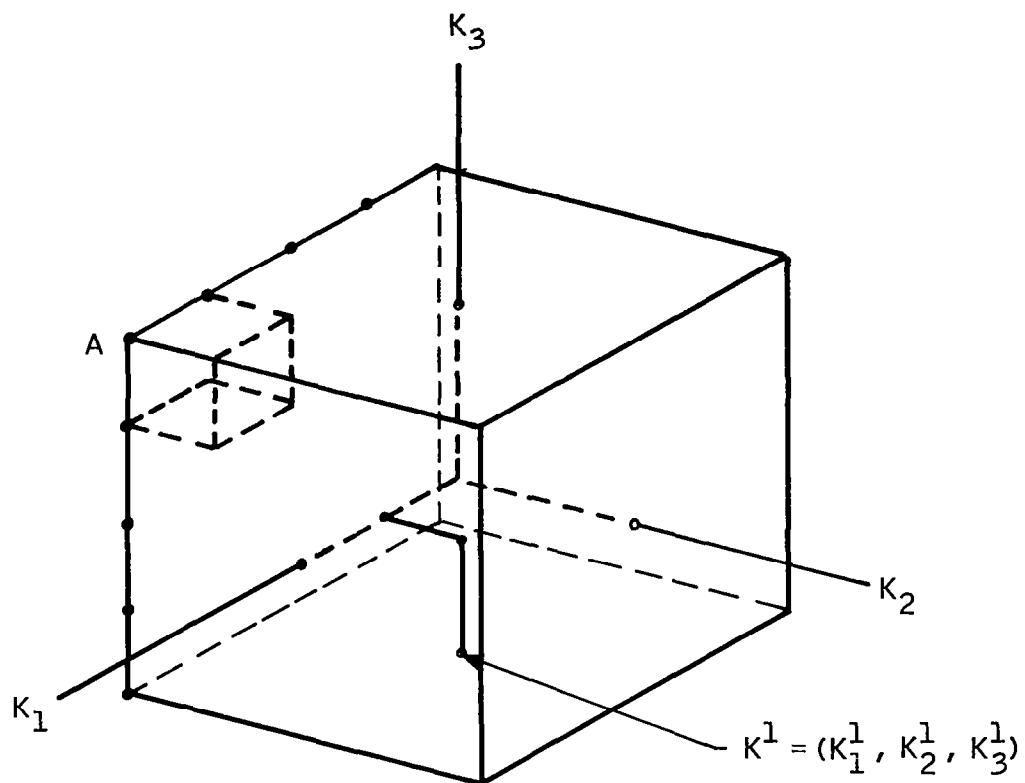
Figure 9. Initial Box of Controllers in Gain Space $\mathcal{K}$

Table 5. Control Costs - Initial Gain Grid

Gain	Values				
K_1	9.2	4.6	0	-4.6	-9.2
K_2	10	5	0	-5	-10
K_3	0.8	0.4	0	-0.4	-0.8

Interval	Cost = $C(K_1, K_2, K_3)$	Interval	
I_1	$C_3(9.2, 10, 0) = 0.02153$ $C_3(9.2, 5, 0) = 0.02155$ $C_3(4.6, 10, 0) = 0.02226$	I_5	$C_3(9.2, 0, 0) = 0.06017$ $C_3(9.2, 10, 0) = 0.06019$ $C_3(9.2, 5, 0) = 0.06019$
I_2	$C_3(9.2, 10, 0) = 0.0736$ $C_3(9.2, 5, 0) = 0.0737$ $C_5(9.2, 0, 0) = 0.1139$	I_6	$C_3(9.2, 10, 0) = 0.1026$ $C_3(9.2, 0, 0) = 0.1026$ $C_3(9.2, 5, 0) = 0.1028$
I_3	$C_3(9.2, 10, 0) = 0.1552$ $C_3(9.2, 5, 0) = 0.1554$ $C_3(9.2, 0, 0) = 0.1562$	I_7	$C_5(4.6, 10, -0.4) = 0.1493$ $C_5(9.2, 10, -0.4) = 0.1575$ $C_5(4.6, 5, -0.4) = 0.1706$ $C_5(9.2, 5, -0.4) = 0.1884$
I_4	$C_3(9.2, 0, 0) = 0.09480$ $C_3(9.2, 10, 0) = 0.09497$ $C_3(9.2, 5, 0) = 0.09502$		

Table 6. Control Costs - Second Gain Grid

Gain	Values				
K_1	13.5	9.0	4.5	0	-4.5
K_2	20	15	10	5	0
K_3	0.7	0	-0.7	-1.4	-2.8

Interval	Cost = $C(K_1, K_2, K_3)$	Interval	
I_1	$C_3(13.5, 20, 0) = 0.02126$ $C_3(13.5, 15, 0) = 0.02127$ $C_3(13.5, 10, 0) = 0.02128$ $C_3(13.5, 5, 0) = 0.02129$	I_5	$C_3(13.5, 20, 0) = 0.06015$ $C_3(13.5, 15, 0) = 0.06015$ $C_3(13.5, 10, 0) = 0.06016$ $C_3(13.5, 5, 0) = 0.06016$ $C_3(13.5, 0, 0) = 0.06016$
I_2	$C_3(13.5, 20, 0) = 0.07265$ $C_3(13.5, 15, 0) = 0.07270$ $C_3(13.5, 10, 0) = 0.07273$ $C_3(13.5, 5, 0) = 0.07277$	I_6	$C_3(13.5, 0, 0) = 0.1010$ $C_3(13.5, 20, 0) = 0.1012$ $C_3(13.5, 15, 0) = 0.1013$ $C_3(13.5, 10, 0) = 0.1014$ $C_3(13.5, 5, 0) = 0.1015$
I_3	$C_3(13.5, 20, 0) = 0.1532$ $C_3(13.5, 15, 0) = 0.1533$ $C_3(13.5, 10, 0) = 0.1534$ $C_3(13.5, 5, 0) = 0.1534$	I_7	$C_5(0, 15, -0.7) = 0.1100$ $C_3(0, 15, -0.7) = 0.1142$ $C_3(4.5, 5, -0.7) = 0.1255$ $C_3(0, 20, -0.7) = 0.1263$
I_4	$C_3(13.5, 20, 0) = 0.09460$ $C_3(13.5, 15, 0) = 0.09463$ $C_3(13.5, 10, 0) = 0.09465$ $C_3(13.5, 0, 0) = 0.99466$ $C_3(13.5, 5, 0) = 0.99467$		

zero was chosen, and the control was on bending moment. Furthermore, the highest of the four or five lowest costs in the grid on the second box were lower than the lowest costs on the grid in the first box.

At this point, these observations were made:

1) Negative values of K_1 and K_2 and to a less marked degree, positive values of K_3 were <u>not</u> used in the best controllers. This was anticipated, but the computations served to verify that a sign reversal had not occurred in selecting the initial point K^1.

2) The low cost controllers contained values of K_1 and K_2 which substantially exceeded those anticipated in choosing K^1.

3) The low cost controllers always had K_3 (the lateral velocity feedback) equal to zero or the negative value nearest zero. Yet the cost was almost always determined by the lateral velocity cost element C_3.

It was concluded that the range of values on K_3 was too broad. A refinement was made by picking a third box of controllers with the same K_1 and K_2 ranges in the second box but with the K_3 dimension reduced by $1/57.3$.* This third box is contained within the second one. Numerical results are in Table 7, and this choice of gain grid is seen to be rewarding in several ways:

1) In the best controllers from the third grid, 65 percent of the values of K_1 and 36 percent of the values of K_2 were on a face of the box. The corresponding numbers for the second box were 82 and 41.

---

*This constant was chosen because not only was the range of K_3 reduced, but also it seemed a convenient check of whether or not values of K_3 had been too large because of an error in dimension. This possibility was subsequently eliminated.

Table 7. Control Costs - Third Gain Grid

Gain	Values					
K_1	13.5	9.0	4.5	0	-4.5	
K_2	20	15	10	5	0	
K_3	·0.0122	0	-0.0122	-0.0245	-0.0489	

Interval	Cost = $C(K_1, K_2, K_3)$	Interval	
I_1	$C_3(13.5, 20, 0) = 0.02126$ $C_3(13.5, 15, 0) = 0.02127$ $C_3(13.5, 10, 0) = 0.02128$ $C_3(13.5, 5, 0) = 0.02129$	I_5	$C_3(0, 0, -0.0245) = 0.03906$ $C_3(0, 0, -0.0122) = 0.05050$ $C_3(0, 5, -0.0489) = 0.05215$ $C_3(-4.5, 15, -0.0489) = 0.05387$
I_2	$C_5(0, 5, -0.0489) = 0.05038$ $C_5(0, 10, -0.0489) = 0.05056$ $C_3(-4.5, 20, -0.0245 = 0.05068$ $C_5(0, 15, -0.0489) = 0.05085$	I_6	$C_3(13.5, 0, -0.0489) = 0.09989$ $C_3(13.5, 20, -0.0489) = 0.09996$ $C_3(13.5, 15, -0.0489) = 0.09999$ $C_3(13.5, 10, -0.0489) = 0.1000$
I_3	$C_3(-4.5, 15, -0.0245) = 0.1125$ $C_3(-4.5, 20, -0.0489) = 0.1307$ $C_3(0, 5, -0.0489) = 0.1329$ $C_3(0, 15, -0.0489) = 0.1443$	I_7	$C_3(13.5, 0, -0.0489) = 0.2253$ $C_3(13.5, 20, -0.0489) = 0.2261$ $C_3(13.5, 15, -0.0489) = 0.2264$ $C_3(13.5, 0, -0.0245) = 0.2264$
I_4	$C_3(0, 0, -0.0245) = 0.07076$ $C_3(0, 0, -0.0489) = 0.07283$ $C_3(-4.5, 10, -0.0489) = 0.07288$ $C_3(-4.5, 5, -0.0245) = 0.07427$		

2) In every interval except the first and seventh, the poorest of the low cost controllers selected in the third grid had lower cost than the best one selected in the second grid. Controllers and costs were the same in the first interval. The good controllers in the seventh interval were poorer with the third grid than with the second, and it was (correctly) anticipated that the lateral velocity $(\dot{Z})$ feedbacks allowed by the small values of K_3 in the third grid were too small compared to the value of $K_3 = -0.4$ which gave the best controllers in the second grid.

3) In the third grid there was more variation from interval to interval in what constituted the best controller than had been true in the first two grids. This was subjectively regarded as a good omen because of the variations in coefficients of the equations of motion from one interval to another.

4) In the low cost controllers from the third grid 60 percent of the values of K_3 were on a (bottom) face of the box for the first time. This indicates that the refinement of values of K_3 in going from the second box to the third was too severe. The first three observations about the third grid still show that refinement of the range of values of K_3 was the correct procedure and that the values of K_3 are apparently rather critical.

COST MAPPING

When the selected gains were all interior to the grids offered, the need for a judicious choice for the range of a given gain grid became pre-eminent. Any technique developed had to recognize the interdependence of each gain on the values of the two remaining.

The five cost elements were plotted as functions of an individual gain with the remaining two gains fixed at their last selected value.

Such a two-dimensional graphing technique permits observing the range of the variable gain which provides the minimum of the maximum costs over the five cost items. Further, it permits subjective selection of that range of the particular gain being considered which should be most competitive when combined with similar ranges of the other two gains. This information can be obtained by observing the rate of change of the maximum cost where it is minimum and determining the corresponding range of the independent gain.

An example of cost mapping is shown in Figure 10. Only the controlling costs items are shown. The remaining costs items would fall substantially below those shown.

In this case, the minimum of the maximum costs occurs on the range $4.75 \le k_2 \le 8.5$, while the competitive range of k_2 might be $4.5 < k_2 < 13.5$. (i.e., $k_3 = C_{min} \pm 10\% \, C_{min}$).

Experience has shown, however, that the upper limit can be lowered appreciably because of the slow rate of change in this portion of the gain range.

Not only is the graph helpful in establishing the range a gain grid should have; it also points out regions within the grid range where trial density should be heavier.

In the example it would be informative to verify the flat cost at $k_2 = 6$ and $k_2 = 7$, and use the three remaining trial values to investigate rising costs near $k_2 \le 4.5$ and $k_2 \ge 8.5$.

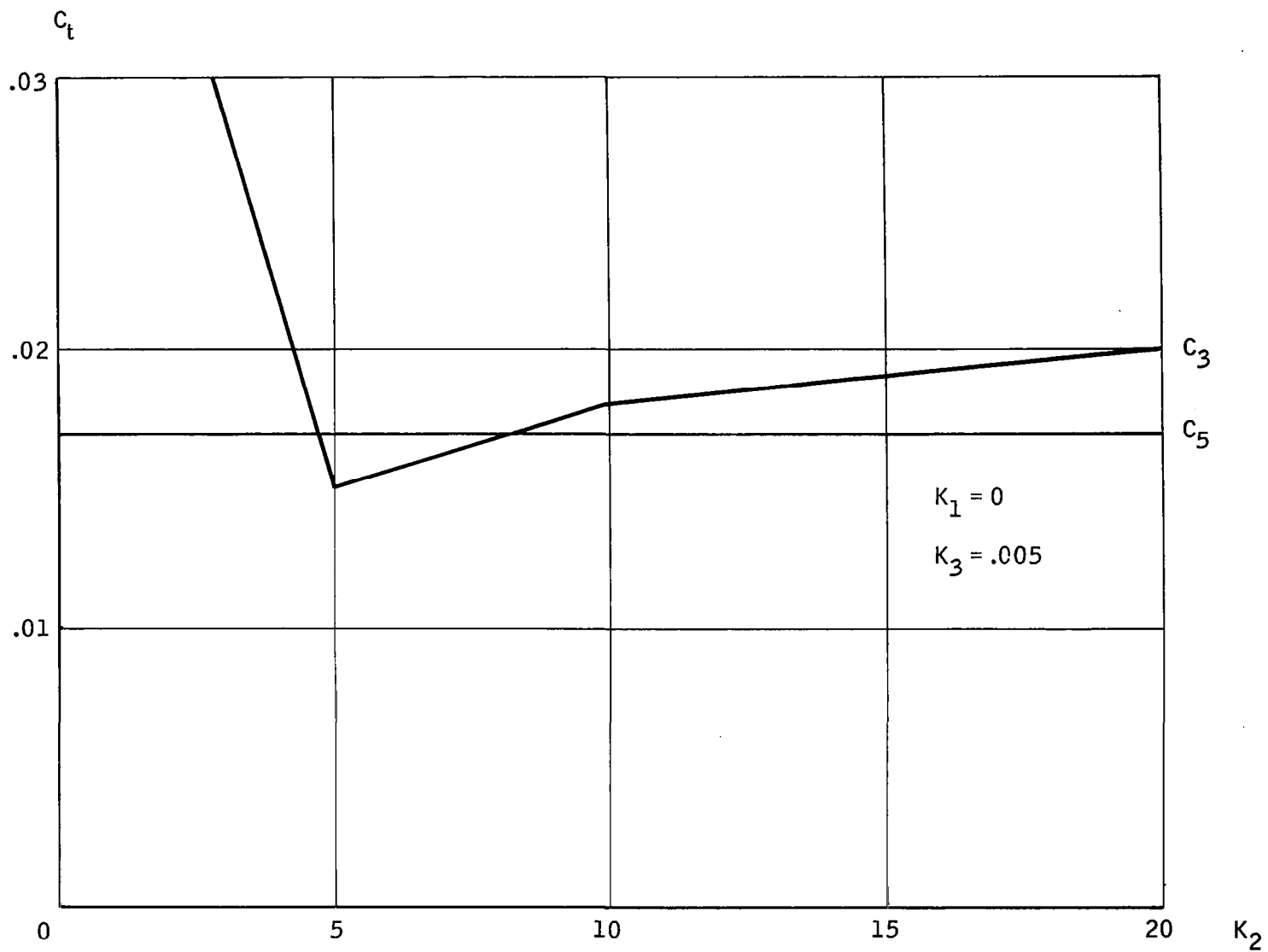Figure 10. Cost Graph

SECTION VII
MINIMAX, DRIFT MINIMUM AND OPEN-LOOP
CONTROLLERS COMPARED

After several iterations of minimax computations, the resulting minimax controllers for each flight interval were compared with the drift-minimum controller for the same interval and with the open-loop controller ($K_1 = K_2 = K_3 = 0$). In all cases, the cost items and weights were those given in Section V under the heading, Weighting Vectors and Scalars Selected.

COMPARISON BASED ON CONTROL COSTS

Table 8 provides a basis for comparing controllers. The last three columns contain respectively the control cost items C_i for the vehicle with "open-loop" control, with drift-minimum control, and with minimax control for each of the seven flight intervals. The first column of numbers repeats the scalar weights D_i from Table 4 assigned to each variable in determining costs. Since the same set of weights were used for each type of controller, the three cost items in any row of Table 8 are proportional to the maximum amplitude of the corresponding cost variable for maximum disturbance inputs (and the common constant of proportionality is the value of D_i in the first column of the same row). Therefore, the performance of controllers for maximum disturbance inputs may be compared by comparing cost items C_i themselves. Results for the vehicle with open loop control are discussed first. In each interval, the largest cost item C_i, hence the cost C, is C_3 (lateral velocity $\dot{Z}$). It exceeds the second largest cost item, which is C_5 (bending moment M_B) in I_4 and I_5 and C_1 (pitch attitude ϕ) in the other intervals, by a factor of at least three. In summary, the uncontrolled vehicle has a lot of drift and "follows its nose" except near Mach 1 (I_4, I_5), where it is more subject to bending. And since the vehicle is uncontrolled, C_4 (gimbal angle β) is zero.

Table 8. Comparison of Controller Costs for Zero Initial Conditions on Each Interval

Interval	$D_i = a \times 10^b$			C_i	Open Loop	Drift-Minimum	Minimax
	i	a	b	i			
I_1	1	0.978	0	1	0.0629	0.00251	0.00103
	2	1.0	-2	2	0.00006	0.00003	0.0000007
	3	0.342	-1	3	C = 0.2074	0.00243	C = 0.01630
	4	0.156	1	4	0	0.04013	0.00208
	5	0.674	-7	5	0.0152	C = 0.07383	0.01625
I_2	1	0.978	0	1	0.1596	0.0096	0.01213
	2	1.0	-2	2	0.0002	0.0001	0.00001
	3	0.342	-1	3	0.4911	0.0104	0.03752
	4	0.156	1	4	0	0.1518	0.01261
	5	0.398	-7	5	0.0269	C = 0.1666	0.03762
I_3	1	0.645	0	1	0.277	0.0152	0.01439
	2	1.0	-2	2	0.001	0.0003	0.00007
	3	0.262	-1	3	C = 1.090	0.0214	0.04605
	4	0.838	0	4	0	C = 0.1835	0.03148
	5	0.166	-7	5	0.043	0.1619	C = 0.04767
I_4	1	0.529	0	1	0.0179	0.0172	0.01609
	2	1.0	-2	2	0.0001	0.0004	0.00007
	3	0.188	-1	3	C = 0.1270	0.0238	0.04673
	4	0.684	0	4	0	C = 0.1870	0.02615
	5	0.120	-7	5	0.0257	0.1576	C = 0.04737
I_5	1	0.499	0	1	0.00364	0.0228	0.03800
	2	1.0	-2	2	0.00002	0.0005	0.00028
	3	0.859	-2	3	0.06336	0.0153	C = 0.03953
	4	0.763	0	4	0	C = 0.2931	0.02824
	5	0.104	-7	5	0.02889	0.1929	0.03790
I_6	1	0.415	0	1	0.0709	0.0156	0.01680
	2	1.0	-2	2	0.0005	0.0004	0.00006
	3	0.143	-1	3	C = 0.2430	0.0235	C = 0.05052
	4	0.608	0	4	0	C = 0.1800	0.03195
	5	0.928	-8	5	0.0428	0.1416	0.05037
I_7	1	0.493	0	1	0.2023	0.0182	0.01806
	2	1.0	-2	2	0.0013	0.0004	0.00017
	3	0.314	-1	3	C = 0.9338	0.0517	0.07738
	4	0.469	0	4	0	0.1443	0.05747
	5	0.1072	-7	5	0.0668	C = 0.1662	C = 0.07878

Notation

$$C_i = D_i \left| y_i \right|_{max}$$

$y_1 = \phi$ rad, $y_2 = \dot{\phi}$ rad/sec, $y_3 = \dot{Z}$ m/sec

$y_4 = \beta$ rad, $y_5 = M_B$ m-kg

The same vehicle with maximum disturbance and a drift-minimum controller of course has low values of C_3. The penalty paid for this is that either C_4 (gimbal angle β) or C_5 (bending moment M_B) cost items are dominant in every interval. Furthermore, the smaller of these two is always at least three times the third highest cost in each interval. Thus the drift-minimum controller calls for large gimbal deflections and causes large bending moments. Large values of each occurred in I_5 and their magnitudes are computed from the data in Table 8 (in the 4th and 5th rows of I_5) as follows:

$$|\beta|_{max} = \frac{0.2931}{0.763} = 0.384 \text{ rad}$$

$$|M_B|_{max} = \frac{0.1929}{0.104 \times 10^{-7}} = 18.5 \times 10^6 \text{ m-kg.}$$

These values are 4.4 times the desired maximum gimbal deflections of 0.087 rad and 6.8 times the desired maximum bending moment of 2.7×10^6 m-kg. However, they correspond to exceedingly severe wind inputs.

The last column of Table 8 contains the costs for the minimax controller for the weights listed in the D column. The first effect of applying the minimax calculations to gain sets successively chosen by the techniques lumped under the name grid mapping is that, in each interval, the highest cost item is reduced and one or more of the other cost items is increased until at least two cost items are approximately equal and greater than the remaining ones. Table 8 illustrates these properties.

To see this, recall that the initial gain-sets were close approximations of the drift-minimum controllers. Then, for each interval, several iterations of cost reduction were effected by choosing successively new gain sets. Note that for the resulting minimax controller, $C_3 \cong C_5$ in every interval. Furthermore, the minimax values of C_3 and C_5 are never as much as half the cost of control for the drift-minimum controller.

Since gimbal deflection and bending moment are large together, it is no surprise that C_4 is usually of the same magnitude as C_5 in the minimax column of Table 8. Furthermore, since the drift-minimum costs have shown low bending moment and low drift to be somewhat antithetical requirements, it can be expected that C_3 and C_5 would be the controlling costs in a design which weighted these two factors heavily.

Finally, interval-5 cost items for the minimax controller correspond to the following maximum values of the cost variables:

$$|\beta|_{max} = \frac{0.02824}{0.763} = 0.037 \text{ rad} < 0.087 \text{ rad.}$$

$$|M_B|_{max} = \frac{0.03790}{0.014 \times 10^{-7}} = 3.64 \times 10^6 \text{ m-kg.}$$

It is seen that the maximum gimbal deflection for this minimax controller is well below the desired value of 0.087 rad and that maximum bending moment is only 1.35 times the desired maximum value. The price paid for this performance is that the maximum lateral velocity in I_5 is 2.6 times as large for this minimax controller as for the drift-minimum controller. It cannot, however, be concluded that drift is 2.6 times as high. It has not been determined (but could be) whether or not the lateral velocity changed sign often, etc. during the response in which it achieved its maximum value.

COMPARISON BASED ON EIGENVALUES

Table 9 lists the gains and eigenvalues of the three types of controllers considered. It is known that drift-minimum controllers have one closed loop pole at the origin. The drift-minimum gains were chosen to give an undamped natural frequency of 0.2 cycles per second and a damping ratio of 0.7. This choice would lead to the two non-zero eigenvalues (closed-loop poles) of $-0.8796 \pm i\, 0.8973$.

The fact that the eigenvalues in the Drift-Minimum column of Table 9 deviate slightly from this indicates minor errors in the drift-minimum gains K_1, K_2, and K_3.

The open loop column of Table 9 shows the eigenvalues of the uncontrolled vehicle in each interval. One positive eigenvalue in each interval shows that the vehicle is asymptotically unstable all the time.

The minimax controllers (last column of Table 9) are seen also to have one positive eigenvalue in each interval; but, except for I_5, this positive eigenvalue is much smaller than for the uncontrolled vehicle. Since bending was weighted heavily in this minimax controller, and since the (stable) drift-minimum controller gave very high bending moments in I_5, it is thought that the relatively large positive closed-loop pole in the minimax controller for I_5 is no accident. That is, in order to minimize bending it may be desirable to use a controller which is not asymptotically stable for a short period of time which includes the event of Mach 1. On the other hand, it is expected that further application of the minimax technique when cost variables have non-zero initial conditions will result in asymptotically stable controllers for most intervals. This aspect of the study will not be considered further in this report.

COMPARISON BASED ON GAINS

A drift-minimum controller is designed to hold rather closely to a given trajectory and has been shown to call for large gimbal deflections and to cause large bending moments. One might guess that a controller which would keep bending moments small would have lower gains than the drift-minimum controller. Figure 11 shows that this is indeed the case for the drift-minimum and minimax controllers having gains listed in Table 9. It should be emphasized, however, that iterative use of the minimax calculations yields values of gains for the (expected) lower gain controller which minimizes the control cost.

Table 9. Comparison of Controller Eigenvalues

|		OPEN LOOP			DRIFT MINIMUM			MINIMAX	
		GAINS	EIGENVALUES		GAINS	EIGENVALUES		GAINS	EIGENVALUES
I_1	K_1	0	.072931,	K_1	4.3	0	K_1	.01	.00522
	K_2	0	-.03739 ±	K_2	5.025	-.88296 ±	K_2	3.0	-.00966
	K_3	0	i.0525	K_3	-.0446	i.85329	K_3	-.0044	-1.1048
I_2	K_1	0	.11387,	K_1	4.26	0	K_1	-.3	.07072
	K_2	0	-.05932 ±	K_2	4.751	-.88006 ±	K_2	4.6	-.01180
	K_3	0	i.06361	K_3	-.204	i.88931	K_3	-.0275	-1.1750
I_3	K_1	0	.15111,	K_1	4.0	0	K_1	.6	.00143
	K_2	0	-.08099 ±	K_2	4.422	-.87997 ±	K_2	3.2	-.22755
	K_3	0	i.04917	K_3	-.514	i.89004	K_3	-.115	-1.0382
I_4	K_1	0	.93331,	K_1	3.68	0	K_1	.28	.01268
	K_2	0	-.05387 ±	K_2	4.099	-.87967 ±	K_2	3.0	-.12597
	K_3	0	i.03396	K_3	-.638	i.88965	K_3	-.11	-1.1651
I_5	K_1	0	.04229,	K_1	3.68	0	K_1	-1.5	.34900
	K_2	0	-.02899 ±	K_2	4.098	-.88063 ±	K_2	3.5	-.01801
	K_3	0	i.01765	K_3	-.867	i.89216	K_3	-.055	-1.1818
I_6	K_1	0	.18582	K_1	3.4	0	K_1	0	.04736
	K_2	0	-.04228	K_2	3.757	-.88026 ±	K_2	3.7	-.04319
	K_3	0	-.15427	K_3	-.805	i.88524	K_3	-.19	-1.7248
I_7	K_1	0	.27290	K_1	3.5	0	K_1	1.25	.00238
	K_2	0	-.03688	K_2	3.756	-.87996 ±	K_2	4.0	-.35442
	K_3	0	-.24546	K_3	-.975	i.89022	K_3	-.475	-1.5106
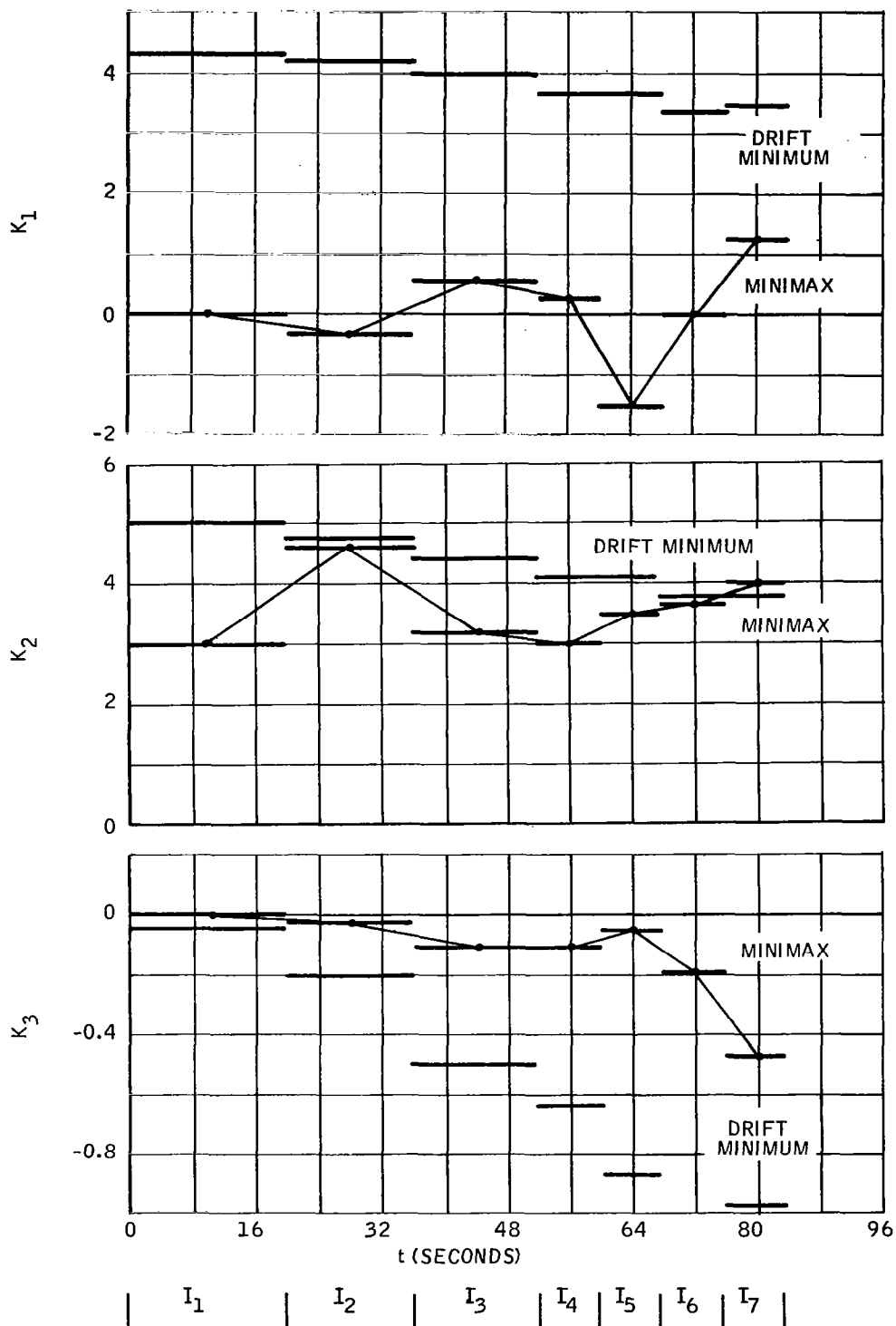
Figure 11.   Controller Gains

SECTION VIII
REDUCTION OF MINIMAX GAIN
CHANGES BETWEEN FLIGHT INTERVALS

Figure 11 shows rather large differences in gains K_1 and K_2 between I_1 and I_2 and between I_2 and I_3. Since the coefficients of the plant all were smooth and monotone throughout I_1, I_2 and most of I_3, it was anticipated that values of K_1 and K_2 in I_2 more in line with those in I_1 and I_3 might lead to lower costs. A set of controllers which were similar to, but with slightly higher costs than the minimax controllers in Figure 11 was selected as the starting point. Figure 12 shows the gains of these selected controllers as the horizontal line segments which are not connected. The values of these gains, the corresponding costs and closed-loop poles are also listed in the left half of Table 10.

The following qualitative comparison of these controllers and the open loop data in adjacent intervals motivated this part of the study.

    A. All coefficients of the open loop equations of motion are monotone throughout I_1, I_2, and almost all of I_3 (Figures 1 through 3 are graphs of these coefficients); but

        1) $K_1 < 0$ in I_2 while $K_1 > 0$ in I_1 and I_3, and

        2) K_2 is much larger in I_2 than in either I_1 or I_3.

    B. Comments similar to those in A for I_2 are applicable for I_5.

    C. In I_5, K_1 has a comparatively large negative value and a closed loop pole at +0.34560. Since the event of Mach 1 occured in I_5, a negative K_1 is not necessarily bad, but further grid mapping might lead to minimax controllers which have lower costs and which are less unstable.
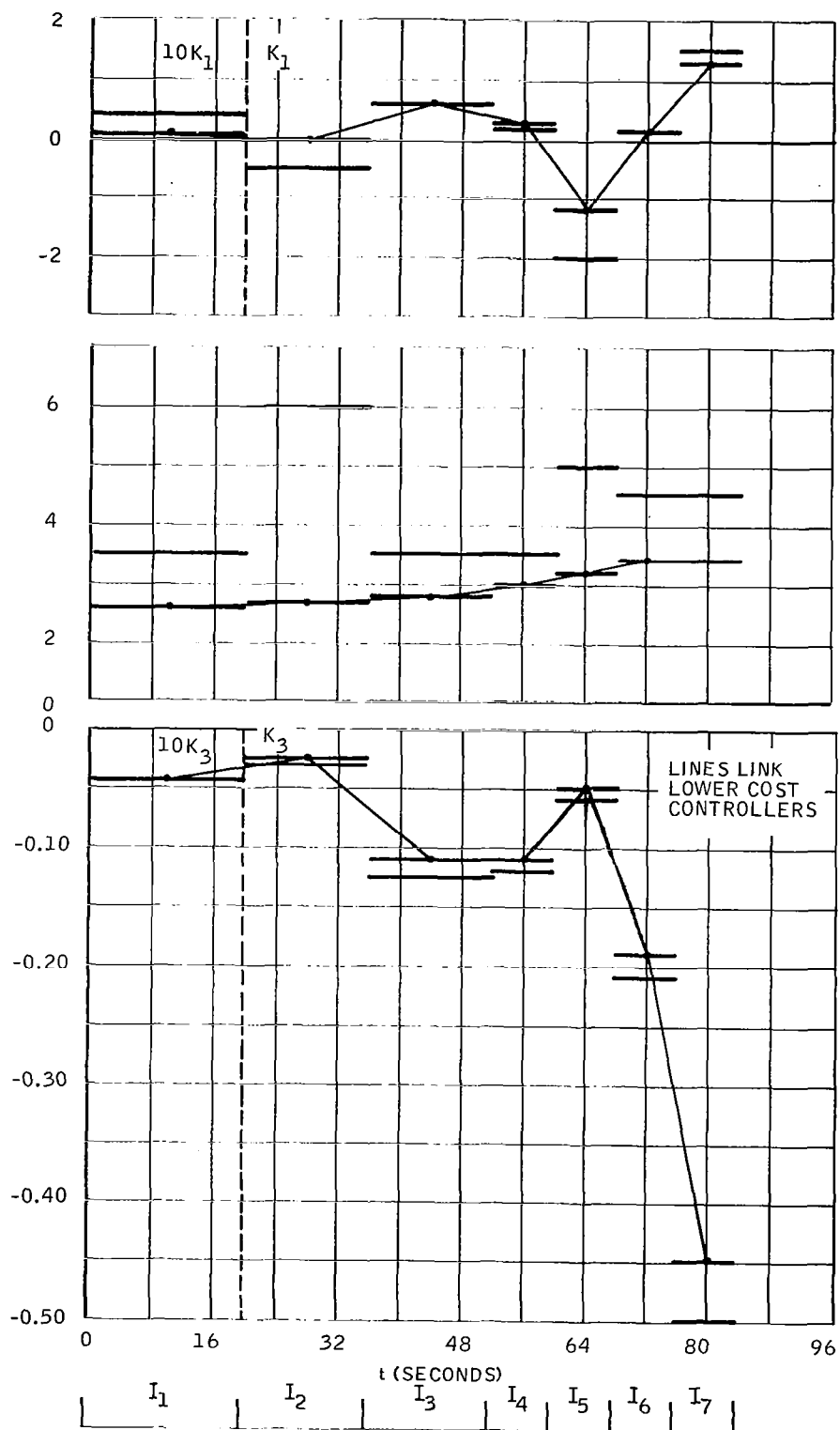
Figure 12. Two Sets of Controllers With Similar Costs

Table 10. Gains, Costs, and Closed-Loop Poles of Controllers in Figure 12

| | INITIAL SET OF CONTROLLERS | | | | | CONTROLLERS WITH REDUCED GAIN CHANGES BETWEEN INTERVALS | | | | |
| | GAINS | | COSTS ($D_2 = 0$) | | POLES | | GAINS | | COSTS | | POLES |
			i	C_i					i	C_i	
I_1	K_1	.04	1	.00107	.00246	K_1	.006	1	.00119	.00640
			2					2	.0000007	
	K_2	3.5	3	.01598	-.01526	K_2	2.6	3	.01566	-.00964
			4	.00219				4	.00204	
	K_3	-.0046	5	C = .01647	-1.2146	K_3	-.0044	5	C = .01624	-.90913
I_2	K_1	-.5	1	.01352	.08648	K_1	0	1	.00967	.02264
			2					2	.000007	
	K_2	6.0	3	.03835	-.01076	K_2	2.7	3	.03580	-.02414
			4	.01410				4	.01125	
	K_3	-.03	5	C = .03902	-2.2798	K_3	-.025	5	C = .03608	-.99438
I_3	K_1	.6	1	.01608	.00313	K_1	.6	1	.01374	.00055
			2					2	.00007	
	K_2	3.5	3	.04815	-.20335	K_2	2.8	3	.04445	-.28190
			4	.03447				4	.03030	
	K_3	-.125	5	C = .05016	-1.1816	K_3	-.11	5	C = .04641	-.82678
I_4	K_1	.2	1	.01701	.02079	K_1	.28	1	.01609	.01268
			2					2	.00007	
	K_2	3.5	3	.04641	-.09269	K_2	3.0	3	.04673	-.12597
			4	.02822				4	.02615	
	K_3	-.12	5	C = .04923	-1.4169	K_3	-.11	5	C = .04737	-1.1651
I_5	K_1	-2.0	1	.03190	.34560	K_1	-1.2	1	.03002	.30809
			2					2	.00020	
	K_2	5.0	3	C = .04001	-.01761	K_2	3.2	3	C = .03939	-.01828
			4	.02746				4	.02084	
	K_3	-.06	5	.03888	-2.4454	K_3	-.050	5	.03863	-1.6509
I_6	K_1	0	1	.01612	.04460	K_1	.15	1	.01587	.02659
			2					2	.00006	
	K_2	4.5	3	.05066	-.04325	K_2	3.4	3	.04959	-.06544
			4	.03579				4	.03214	
	K_3	-.21	5	C = .05261	-2.0912	K_3	-.19	5	C = .05017	-1.5435
I_7	K_1	1.5	1	.01611	.00067	K_1	1.3	1	.01686	.00076
			2					2	.00018	
	K_2	4.5	3	.08109	-.37924	K_2	3.4	3	.07417	-.51510
			4	.06083				4	.05525	
	K_3	-.50	5	C = .08129	-1.7151	K_3	-.45	5	C = .07525	-1.0713

ew gain-grids were chosen for each interval with a veiw to reducing costs
nd reducing gain changes between intervals. This first iteration of minimax
omputations met with substantial success in the two worst intervals (I_2 and I_5).
he results at this stage were the controllers which were compared with the
rift minimum controllers in Section VII. The corresponding gains, costs, and
igenvalues are found in Figure 11 and Tables 8 and 9. One more iteration of
rid mapping was done in all intervals and two more were done in I_2, I_4, and
. A general trend was that each successive gain grid contained three or more
ontrollers which had lower costs than the best controller in the previous grid
or that interval. The control cost reductions ranged from about one-half to
ve percent each time with most reductions in the neighborhood of three percent.
he closed-loop pole locations did not follow an unbroken trend. The final sets
f controllers each had one positive eigenvalue, but it was less positive than
ie corresponding eigenvalue for the starting set of controllers in all intervals
xcept I_1 and I_7. The gains, costs, and eigenvalues of the set of controllers
here this study was terminated are shown in the right half of Table 10. These
ains are shown graphically in Figure 12 as the horizontal line segments with
onnected midpoints. It is seen that the large fluctuations in K_2 have been
liminated and that K_2 is monotone increasing in the final set of controllers.
he negative K_1 was eliminated in I_2 and was reduced in magnitude by 40
ercent in I_5. Furthermore, the changes in gains between intervals were
educed in almost every case, so that all three gain "curves" are smoother
ian the initial ones.

he total cost reductions in each interval were as follows:

Interval	Cost Reduction (percent)
I_1	1.4
I_2	8.1
I_3	8.0
I_4	3.9
I_5	1.5
I_6	4.8
I_7	8.01

It should also be mentioned that the best controller found for I_4 in the grid mapping described in this section had control cost four percent lower than the controller actually shown in Figure 12 and Table 10. The higher-cost-controller was selected since it fit better into the demonstrations of gain change reduction, which was the purpose of this section. The lower-cost-controller is defined by K = (0.25, 0.20, -0.095). It is seen that this would cause a sharp break in the K_2 curve at I_4 in Figure 12.

The question arises as to whether or not one could achieve a reasonably smooth set of controller gains at a lower cost level. There is reason to believe that one could, since six of the lower-cost-controllers shown in Figure 12 occurred on a face or an edge of the box of controllers spanned by this grid. However, the cost reductions with each iteration of grid mapping are now slight and the ability to achieve gain smoothing without increasing costs has been demonstrated.

SECTION IX
RESTRICTIONS ON THE CLASS OF
ALLOWABLE CONTROLLERS

The class of allowable controllers considered in this report is given by (2), and for the specific example by (10). It is a class of linear controllers with fixed gains over finite time intervals. It might be desired that further restrictions be placed on the class from which controllers are to be selected. In Section VII, Tables 8 and 9, two extremes were observed. The minimax controllers were selected solely on the basis of minimizing control cost in each (finite) flight interval. The resulting controllers all were asymptotically unstable, though only slightly so in all intervals except the fifth one. The drift minimum controllers were totally specified by the conditions that the controllers be drift minimum and have an undamped natural frequency of 0.2 cycles per second with a damping ratio of 0.7. Minimax computations showed these controllers to have substantially higher costs than the minimax controllers in each flight interval.

It would be practical to impose conditions on the class of controllers which are intermediate between the two extremes of only cost minimization and total specification; however, imposing such restrictions would usually increase control costs. Examples of increasing degrees of restriction for controllers of the launch booster defined in Section III will serve as illustrations.

DRIFT-MINIMUM PRINCIPLE IMPOSED

The characteristic equation of the closed loop plant will be written as:

$$\lambda^3 + A_1 \lambda^2 + A_2 \lambda + A_3 = 0 \tag{28}$$

where, in the notation of Tables 1 and 2,

$$A_1 = - \left[\left(a_{33} + b_3 K_3 \right) \frac{1}{V} + b_2 K_2 \right] \tag{29}$$

$$A_2 = \left[\left(a_{33} b_2 - a_{23} b_3 \right) \frac{1}{V} K_2 - \left(a_{21} + b_2 K_1 \right) \right] \tag{30}$$

$$A_3 = \frac{1}{V} \left[\left(a_{33} b_2 - a_{23} b_3 \right) K_1 + \left(a_{21} b_3 - a_{31} b_2 \right) K_3 \right. $$
$$\left. + \left(a_{21} a_{33} - a_{23} a_{31} \right) \right] \tag{31}$$

The drift minimum principle is defined by requiring $\ddot{Z} = 0$ when ϕ is quasi-steady state. It can be shown that this is equivalent to $A_3 = 0$, and it is clear from (28) that one closed-loop pole is then at the origin ($\lambda = 0$). Thus, setting (31) equal to zero gives a linear equation in k_1 and k_3 which must be satisfied to give a drift-minimum controller. Two gains remain unspecified, and iterations of minimax calculations (subject to $A_3 = 0$) could be used to find a minimax drift-minimum controller.

A further restriction on the class of controllers defined by (10) would be to impose the drift-minimum principle and require that the two unspecified pole locations be in the left half-plane. Then one would consider minimax controllers which satisfy $A_3 = 0$ and the conditions specified in (32).

$$A_1 > 0$$
$$\tag{32}$$
$$A_2 > 0$$

It is seen by referring to (29) and (30) that (32) gives two linear inequalities which must be satisfied by the controller gains.

ASYMPTOTIC STABILITY IMPOSED

A still more restricted subclass of (10) would be controllers which are asymptotically stable. It can be shown that conditions (32) and (33) are necessary and that these, together with (34) are sufficient for asymptotic stability.

$$A_3 > 0 \tag{33}$$

$$A_1 A_2 > A_3 \tag{34}$$

Note that such a controller can still be arbitrarily close to being drift-minimum by having A_3 be sufficiently small. Minimax calculations would still be applicable in arriving at stable-minimax controllers.

SECTION X
CONCLUSIONS

Optimal control theory has been applied to a piecewise constant approximation of a large launch booster for the first 84 seconds of flight. This period was divided into seven intervals with a different constant approximation of the vehicle in each interval. The controllers considered are linear controllers with constant gains in each flight interval. The disturbances are the cross-winds of bounded amplitude which cause the maximum of any of several cost items to occur in each flight interval, and each cost item is proportional to some physical quantity of interest. The cost of a given controller is the maximum of its several cost items.

The optimal control theory is presented in the appendix. In Section II, it is summarized and extended so that cost items whose corresponding physical quantity depends explicitly on the disturbances may be considered. This extension was necessary to consider a bending moment cost item.

The theory provides a straightforward method of computing the cost of a finite set of controllers. The minimum-cost controller of the set is called the minimax controller of that set. It will usually be a sub-optimal controller since the cost computations (called minimax computations) are performed for only a finite set of controllers.

Bending moment is weighted heavily in the cost items for the minimax computations. A comparison of control costs for specific drift-minimum controllers and minimax controllers is presented. It is found that, for the severe disturbances considered, drift-minimum controllers give excessive bending moments and gimbal deflections. Of course, they have low lateral velocities. The minimax controllers have acceptable gimbal angles, maximum bendings

moments which are nearly acceptable, and maximum lateral velocities which exceed those of the drift-minimum controller by a factor of only about 2.5.

It is shown that one can impose "classical" design criteria (e. g., asymptotic stability) on the class of controllers to be considered and still use minimax computations to specify remaining control parameters.

APPENDIX
MINIMAX CONTROL OF LINEAR STATIONARY SYSTEMS WITH NONZERO INITIAL CONDITIONS AND AMPLITUDE BOUNDED DISTURBANCES

by

C. A. HARVEY

ABSTRACT

The design of an optimal controller with respect to a class of load disturbances is the problem which motivates this study. One result concerning this problem is presented here. It is assumed that the plant is represented by linear stationary equations of motion. A class of linear fixed-gain controllers is assumed as the class of allowable controllers and the class of possible disturbances is assumed to be all disturbances which are uniformly bounded. For any given initial condition a method is presented for the computation of the performance index of any allowable controller. This result requires the integration of a system of piece-wise linear differential equations and the monitoring of the time history of the amplitude of certain piece-wise linear combinations of the components of the solutions to these differential equations.

INTRODUCTION

A technical statement of the problem considered is given, and the proposed method of solution is briefly described in the PROBLEM STATEMENT. The major result is then developed in the DERIVATION OF COMPUTATIONAL METHOD.

The special case when the initial condition was given to be zero and the class of admissible disturbances was all disturbances of uniformly bounded magnitude had been solved previously. The more general problem presented here has a somewhat more complicated but similar solution. The complication appears in two ways. First, there are additional linear homogeneous differential equations to be integrated. The other complication is the necessity of monitoring the time history of amplitudes of functions of the solution of the differential equations to ascertain the maximum amplitude attained on the time interval of interest.

PROBLEM STATEMENT

The following optimal control problem is considered. It is assumed that the plant is represented by the vector differential equation

$$\dot{x} = Ax + Bu + Cg, \quad x(0) = x^O \tag{1}$$

where x is an n-vector describing the state of the system, x^O is the given initial condition, u is an m-vector representing the control inputs and g is a k-vector representing the disturbance inputs. A, B and C are constant matrices of appropriate sizes. Classes of allowable controllers and disturbances are assumed to be as follows: Ω is a class of linear fixed-gain controllers, i.e., $u \in \Omega$ if $u = Qx + Rg$ with Q and R satisfying certain restrictions; G is defined by

$$G = \left\{ g(t) : \ a_i \le g_i(t) \le b_i, a_i \le b_i, \ i=1, 2, \ldots, k; \ 0 \le t \le T, g(t) \ \text{measurable} \right\}$$

The requirements on Q and R may be specified by such considerations as; gain magnitude restrictions, sensor restrictions, stability requirements, etc.

To define the performance index it is assumed that constant n-vectors $d(i)$, $i = 1, 2, \ldots, s$ are given. For $u \in \Omega$, the cost functional $C(u)$ is defined as

$$C(u) = \max_{1 \leq i \leq s} C_i(u)$$

where $\quad C_i(u) = \max_{0 \leq t \leq T} \max_{g \in G} \left| d(i) \cdot x(t; x^O, u, g) \right|, \quad i = 1, 2, \ldots, s,$

with $x(t; x^O, u, g)$ representing the solution to (1). An optimal controller is a $u \in \Omega$ which minimizes $C(u)$.

It is desired to find an optimal controller. As a means toward this end a method will be developed by which $C_i(u)$ may be readily computed for any $u \in \Omega$. This makes it feasible to compute $C(u)$ for any $u \in \Omega$. Then for a finite set of controllers Δ that spans Ω, $C(u)$ could be computed for each $u \in \Delta$. The optimal controller with respect to Δ then provides an approximation to an optimal controller with respect to Ω.

The major step is the method of computation of $C_i(u)$. This will now be developed.

DERIVATION OF COMPUTATIONAL METHOD

Assume $u = Qx + Rg$ and let A_Q and C_R denote the matrices $A + BQ$ and $C + BR$ respectively. Also let h denote the k-vector with components $h_j = (a_j + b_j)/2$. Then for any vector $d(i)$ the following equation may be obtained from the variation of parameters formula for the solution of (1).

$$
\begin{aligned}
d(i) \cdot x(t; x^O, u, g) = d(i) \cdot e^{A_Q t} x^O + \int_0^t d(i) \cdot e^{A_Q(t-\tau)} C_R h \, d\tau \\
+ \int_0^t d(i) \cdot e^{A_Q(t-\tau)} C_R \left[g(\tau) - h \right] d\tau \quad (2)
\end{aligned}
$$

Let $\lambda_i(t) = d(i) \cdot e^{A_Q t} x^0 + \int_0^t d(i) \cdot e^{A_Q(t-\tau)} C_R h \, d\tau$ and set

$\mu_i(t, \gamma) = \int_0^t d(i) \cdot e^{A_Q(t-\tau)} C_R \gamma(\tau) d\tau$ with $\gamma(\tau) = g(\tau) - h$. Then $|\gamma_j(\tau)| \leq \frac{1}{2}(b_j - a_j)$.

Also let $\mu_i(t) = \mu_i\left[t, \gamma(\tau, i)\right]$ where the jth component of $\gamma(\tau, i)$ is given by

$$\gamma_j(\tau, i) = \frac{1}{2}(b_j - a_j) \operatorname{sgn}\left[d(i) \cdot e^{A_Q(t-\tau)} C_R(j)\right] \text{ with}$$

$C_R(j)$ denoting the jth column of C_R and note that $h + \gamma(\tau, i)$ and $h - \gamma(\tau, i)$ belong to G. The maximizing and minimizing elements of G for the functional $\mu_i(t, \gamma)$ correspond to the functions plus and minus $\gamma(\tau, i)$ respectively. To verify this it is noted that

$$\mu_i(t) = \frac{1}{2} \sum_{j=1}^{k} (b_j - a_j) \int_0^t |d(i) \cdot e^{A_Q(t-\tau)} C_R(j)| \, d\tau$$

and hence

$$\mu_i(t) - \mu_i(t, \gamma) = \frac{1}{2} \sum_{j=1}^{k} (b_j - a_j) \int_0^t \left\{ |d(i) \cdot \varphi(j, t-\tau)| - d(i) \cdot \varphi(j, t-\tau) \left[\frac{\gamma_j(\tau)}{b_j - a_j}\right] \right\} d\tau$$

where

$$\varphi(j, t-\tau) = e^{A_Q(t-\tau)} C_R(j)$$

and $\left|\dfrac{\gamma_j(\tau)}{b_j - a_j}\right| \leq \frac{1}{2}$ for each $g \in G$. Each integrand is non negative

and hence $\mu_i(t) \geq \mu_i(t, \gamma)$ which together with the fact that $\mu_i(t, -\gamma) = -\mu_i(t, \gamma)$ gives the desired result that

$$-\mu_i(t) \leq \mu_i(t, \gamma) \leq \mu_i(t) \quad \text{for any } g \in G.$$

From the expression for $\mu_i(t)$ it is clear that $\mu_i(0) = 0$ and $\mu_i(t)$ is **monotone** nondecreasing in t.

Now it is clear that

$$\max_{g \in G} |d(i) \cdot x(t; x^0, u, g)| = \max_{g \in G} |\lambda_i(t) + \mu_i(t, g)|$$

and it will be established that

$$\max_{g \in G} |\lambda_i(t) + \mu_i(t, g)| = |\lambda_i(t)| + \mu_i(t)$$

Clearly, $\max_{g \in G} |\lambda_i(t) + \mu_i(t, g)| \leq \max_{g \in G} \left\{ |\lambda_i(t)| + |\mu_i(t, g)| \right\} = |\lambda_i(t)| + \mu_i(t)$.

If $\lambda_i(t) \geq 0$, $|\lambda_i(t) + \mu_i(t)| = |\lambda_i(t)| + \mu_i(t)$ and if $\lambda_i(t) < 0$,

$|\lambda_i(t) - \mu_i(t)| = |-\lambda_i(t) + \mu_i(t)| = |\lambda_i(t)| + \mu_i(t)$ and hence there

is a $g \in G$ such that $|\lambda_i(t) + \mu_i(t, g)| = |\lambda_i(t)| + \mu_i(t)$ which

establishes the desired result.

$$\text{Thus } C_i(u) = \max_{t \in 0, T} \left\{ |\lambda_i(t)| + \mu_i(t) \right\}. \text{ It will next be}$$

shown that $\lambda_i(t)$ and $\mu_i(t)$ may be obtained as solutions of differential equations. As solutions are generated by numerically integrating the differential equations it is easy to generate the time function, $|\lambda_i(t)| + \mu_i(t)$ and monitor it on the interval $0 \leq t \leq T$ to determine the maximum value attained there.

Let $p(t)$, $q(t)$, $r(t, j)$, $j = 1, 2, \ldots, k$ be solutions of the differential equation $\dot{y} = A_Q y$ which satisfy $p(0) = x^0$, $q(0) = C_R h$,
$r(0, j) = \frac{1}{2}(b_j - a_j) C_R(j)$. Also let $\dot{v}_i(t) = d(i) \cdot q(t)$, $v_i(0) = 0$ and

$\dot{w}_i(t) = \sum_{j=1}^{k} |d(i) \cdot r(t, j)|$, $w_i(0) = 0$, $i = 1, 2, \ldots, s$. Then $\lambda_i(t) = d(i) \cdot p(t) + v_i(t)$

and $\mu_i(t) = w_i(t)$. Thus everything necessary for the computation of $C(u)$

may be obtained by integrating n(k+2) + 2s first order differential equations, all but s of which are linear and the remaining s are piecewise linear. The required integration can readily be carried out on a high speed computer.

CONCLUSIONS

A computational procedure is presented which may be used to find an approximation to the optimal controller for linear constant coefficient systems having a nonzero initial condition when the system is subjected to a class of load disturbances that are bounded in amplitude. The procedure requires the integration of an autonomous piece-wise linear system of differential equations and monitoring the magnitude of piece-wise linear combinations of component of the solution to the differential equation system.

"The aeronautical and space activities of the United States shall be conducted so as to contribute . . . to the expansion of human knowledge of phenomena in the atmosphere and space. The Administration shall provide for the widest practicable and appropriate dissemination of information concerning its activities and the results thereof."

—NATIONAL AERONAUTICS AND SPACE ACT OF 1958

NASA SCIENTIFIC AND TECHNICAL PUBLICATIONS

TECHNICAL REPORTS: Scientific and technical information considered important, complete, and a lasting contribution to existing knowledge.

TECHNICAL NOTES: Information less broad in scope but nevertheless of importance as a contribution to existing knowledge.

TECHNICAL MEMORANDUMS: Information receiving limited distribution because of preliminary data, security classification, or other reasons.

CONTRACTOR REPORTS: Technical information generated in connection with a NASA contract or grant and released under NASA auspices.

TECHNICAL TRANSLATIONS: Information published in a foreign language considered to merit NASA distribution in English.

TECHNICAL REPRINTS: Information derived from NASA activities and initially published in the form of journal articles.

SPECIAL PUBLICATIONS: Information derived from or of value to NASA activities but not necessarily reporting the results of individual NASA-programmed scientific efforts. Publications include conference proceedings, monographs, data compilations, handbooks, sourcebooks, and special bibliographies.

Details on the availability of these publications may be obtained from:

SCIENTIFIC AND TECHNICAL INFORMATION DIVISION

NATIONAL AERONAUTICS AND SPACE ADMINISTRATION

Washington, D.C. 20546